The Linnean Society of London ZOOLOGICAL Journal of the Linnean Society

Zoological Journal of the Linnean Society, 2009, **156**, 465–493. With 11 figures

Morphological and molecular description of new species of squat lobster (Crustacea: Decapoda: Galatheidae) from the Solomon and Fiji Islands (South-West Pacific)

PATRICIA CABEZAS[1]*, ENRIQUE MACPHERSON[2] and ANNIE MACHORDOM[1]

[1]*Museo Nacional de Ciencias Naturales (CSIC), José Gutiérrez Abascal 2, 28006 Madrid, Spain*
[2]*Centro de Estudios Avanzados de Blanes (CSIC), Carr. Acc. Cala Sant Francesc 14, 17300 Blanes, Girona, Spain*

Received 31 March 2008; accepted for publication 19 June 2008

The family Galatheidae is among the most diverse families of anomuran decapod crustaceans, and the South-West Pacific is a biodiversity hot spot for these squat lobsters. Attempts to clarify the taxonomic and evolutionary relationships of the Galatheidae on the basis of morphological and molecular data have revealed the existence of several cryptic species, differentiated only by subtle morphological characters. Despite these efforts, however, relationships among genera are poorly understood, and the family is in need of a detailed systematic review. In this study, we assess material collected in different surveys conducted in the Solomon Islands, as well as comparative material from the Fiji Islands, by examining both the morphology of the specimens and two mitochondrial markers (cytochrome oxidase subunit I, COI, and 16S rRNA). These two sources of data revealed the existence of eight new species of squat lobster, four of which were ascribed to the genus *Munida*, two to the genus *Paramunida*, one to the genus *Plesionida*, and the last species was ascribed to the genus *Agononida*. These eight species are described along with phylogenetic relationships at the genus level. Our findings support the taxonomic status of the new species, yet the phylogenetic relationships are not yet fully resolved. Further molecular analysis of a larger data set of species, and more conserved genes, will help clarify the systematics of this group. *Zoological Journal of the Linnean Society*, 2009, **156**, 465–493.

ADDITIONAL KEYWORDS: 16S rRNA gene – COI gene – decapoda – molecular systematics – morphology.

INTRODUCTION

Squat lobsters of the family Galatheidae Samouelle, 1819 are among the most diverse families of anomuran decapod crustaceans, and their distribution includes all marine habitats, except polar regions, with a hot-spot of biodiversity in the Indo-West Pacific (Baba, 2005). This area has received the greatest taxonomic attention in the last few decades (Baba, 1988; Macpherson, 1994; Baba, 2005; Macpherson & Baba, 2006; Macpherson, 2006a), and numerous new species have been described as a result of the large sampling effort. At present, the family contains 33 genera, with the most widely represented decapod taxa in these waters being ascribed to the genus *Munida* Leach, 1820 and closely related genera. In effect, more than 250 species of these genera have been cited for the area (Baba, 2005, and references cited therein). Despite the fact that the galatheoid fauna is well known in many areas of the South-West Pacific, e.g. New Caledonia (Macpherson, 1994, 1996, 2006b), Fiji and Tonga (Baba, 1995); (Macpherson, 2004), eastern Australia (Ahyong & Poore, 2004), and New Zealand (Ahyong, 2007), this biota has been barely studied in the Solomon Islands. Most studies carried out in the waters of the Solomon Islands have focused on shallow waters (Challis, 1969; Miller,

*Corresponding author. E-mail: pcabezas@mncn.csic.es

1969; Wolff, 1969; Bruce, 1980; Blaber & Milton, 1990), and those examining deep-sea faunas (Macpherson, 2003; Goggin, 2004; Castro, 2005; Ahyong & Galil, 2006; Cleva & Crosnier, 2006; Galil, 2007) have provided no information on galatheoid fauna.

The evolution of these squat lobsters seems to be marked by rapid speciation, and stasis during the Miocene, with some genera (e.g. *Munida*, *Paramunida*, and *Raymunida*) being monophyletic, according to both morphological and molecular data, and others (e.g. *Agononida* and *Crosnierita*) appearing as poly- or paraphyletic (Machordom & Macpherson, 2004). Knowledge of the phylogeny of the group is still scarce, and more data are needed to clarify the taxonomy and evolution of the different genera. Here, we describe a number of new species of the genera *Agononida*, *Munida*, *Paramunida*, and *Plesionida* for the area, based on both morphological and molecular information. This was necessary because diagnostic characters in the family Galatheidae and other decapod families are often based on subtle morphological differences. The use of additional information sources, such as molecular tools, is therefore strongly recommended. We selected two mitochondrial markers, the cytochrome oxidase subunit I (COI) gene and the 16S rRNA gene. These genes have been previously used to elucidate phylogenetic relationships at the genus and species level in this family (Lin, Chan & Chu, 2004; Cubelio *et al.*, 2007; Cabezas, Macpherson & Machordom, 2008), and in other decapod crustaceans, such as the family Palinuridae (Groeneveld *et al.*, 2007).

We examined specimens of the family Galatheidae collected during expeditions to the Solomon Islands (designated SALOMON 1 and SALOMON 2), and also re-examined material collected in surveys conducted in Fiji (MUSORSTOM 10 and BORDAU 1) and in New Caledonia (HALIPRO 1, HALIPRO 2 and BATHUS 1). This work represents the first record of the genera *Munida*, *Paramunida*, *Plesionida* and *Agononida* for the Solomon Islands.

Here, we describe and illustrate seven new species from the Solomon Islands: one species belonging to the genus *Agononida*, one to the genus *Plesionida*, two to the genus *Paramunida*, and three to *Munida*. A further species ascribed to the genus *Munida*, closely related to one of the above new species, is described for the region of Fiji. Molecular data are used to increase the knowledge on the phylogenetic relationships of the genera. Both the morphological and molecular data support the taxonomic status of the new species.

MATERIAL AND METHODS

Sampling and identification

Specimens were collected using beam trawls or Waren dredges in expeditions to the Solomon Islands conducted in September–October 2001 (SALOMON 1) and October–November 2004 (SALOMON 2). For comparative purposes, we also examined some specimens from Fiji and New Caledonia (Table 1). The material examined was deposited in the collections of the Muséum National d'Histoire Naturelle, Paris (MNHN). Measurements of specimens represent the postorbital carapace length. The terminology used mainly follows Zariquiey Alvarez (1952), Baba & de Saint Laurent (1996) and Baba (2005). Following Baba (2005), the terms flexor and extensor borders of

Table 1. Squat lobster species examined genetically, and the corresponding sample size, locality, station, depth, and survey label

Species	*N*	Locality	Station	Depth (m)	Survey
***Agononida isabelensis* sp. nov.**	2	Solomon Islands	Stn 2210	240–347	SALOMON 2
***Paramunida lophia* sp. nov.**	3	Solomon Islands	Stn 1831/2199	135–325	SALOMON 1/2
***Paramunida salai* sp. nov.**	3	Solomon Islands	Stn 1831	135–325	SALOMON 1
Paramunida proxima	1	Solomon Islands	Stn 1831	135–325	SALOMON 1
Paramunida stichas	2	Solomon Islands	Stn 1831	135–325	SALOMON 1
***Plesionida concava* sp. nov.**	2	Solomon Islands	Stn 2260	399–427	SALOMON 2
***Munida oblongata* sp. nov.**	1	Solomon Islands	Stn 2297	728–777	SALOMON 2
***Munida mendagnai* sp. nov.**	2	Solomon Islands	Stn 1825/1826	340–432	SALOMON 1
***Munida caeli* sp. nov.**	2	Solomon Islands	Stn 1801/1802	245–271	SALOMON 1
Munida delicata	1	Solomon Islands	Stn 2263	485–520	SALOMON 2
Munida leagora	2	Solomon Islands	Stn 2202	304–395	SALOMON 2
***Munida lailai* sp. nov.**	1	Fiji Islands	Stn 1348	327–420	MUSORSTOM 10/BORDAU 1
Munida parca	2	New Caledonia	Stn 687/851	314–440	BATHUS 1/HALIPRO 1
Munida devestiva	1	New Caledonia	Stn 60	1133–1280	HALIPRO 2

articles are only used for the maxilipeds and dactyli of the walking legs. The abbreviations used in the text are as follows: F, female; juv., juvenile; M, male; Mxp, maxiliped; ovig., ovigerous; P1, pereiopod 1, cheliped; P2–P4, pereiopods 2–4, first to third walking legs.

DNA EXTRACTION, AMPLIFICATION, AND SEQUENCING

Total DNA was extracted from tissue samples using the magnetic Charge Switch gDNA Micro Tissue Kit (Invitrogen). Fragments of the COI and 16S rRNA genes were amplified by polymerase chain reaction (PCR). Primers used for the amplification of COI were COIH (Machordom & Macpherson, 2004), six bases shorter than HCO2198 from Folmer *et al.* (1994), and the newly designed primers ParaCOIF 5′-GGMGC HTGRGCHGGHATAG-3′ and ParaCOIR1 5′-GGRTC TCCWCCWCCDGCRGGRTC-3′. Unfortunately, some specimens belonging to the genus *Munida* yielded no results in the COI amplification. The 16S rRNA fragment was amplified using the primers L12 5′-TGA CCGTGCAAAGGTAGCATAA-3′ (Schubart, Diesel & Hedges, 1998) and 16SBR 5′-CCGGTCTGAACTCAG ATCACGT-3′ (Palumbi *et al.*, 1991).

Reactions were prepared in a final volume of 50 μL, and the PCR mix contained 2 μL of DNA template, 0.16 μM of both primers, 0.2 mM of each deoxyribonucleotide triphosphate (dNTP), 5 μL of buffer (containing a final concentration of 2 mM $MgCl_2$), 0.5 μL of bovine serum albumin (BSA; 10 mg mL^{-1}), 1.5 U of Taq DNA polymerase (Biotools) and double-distilled water (ddH_2O). The amplification process for the 16S rRNA sequence was conducted as follows: 94 °C (4 min), 40 cycles at 94 °C (45 s), 45 °C (1 min), 72 °C (1 min), and a final extension at 72 °C (10 min). Amplification of the COI gene was performed under the same conditions, except for a higher annealing temperature (50 °C).

The amplified fragments, 526 bp for the 16S rRNA gene and 657 bp for the COI gene, after removing primer regions, were purified by ethanol precipitation prior to sequencing both strands using 'Big Dye Terminator' (Applied Biosystems, ABI). Sequences were run on an ABI 3730 Genetic Analyzer (Applied Biosystems). Forward and reverse DNA sequence strands were compared using the Sequencher program (Gene Code) after removing the primer regions. New sequences were deposited in GenBank under accession numbers EU417965–EU418012.

PHYLOGENETIC ANALYSES

The 16S rRNA and COI sequences were checked using the program Sequencher (Gene Code), and alignment was performed by hand using the program PAUP* v4.0 b10 (Swofford, 2002). All analyses were performed separately for each of the genera *Agononida*, *Munida*, and *Paramunida* (except for the genus *Plesionida*, which was jointly analysed with the genus *Paramunida*, as only two species of the genus were examined). The evolutionary molecular model that best fitted our data was selected using ModelTest 3.7 (Posada & Crandall, 1998) and the Akaike's Information Criterion (Akaike, 1974). Phylogenetic analyses were conducted for each gene data set, and for the combined data set, using the following software: MrBayes v3.0B4 (Huelsenbeck & Ronquist, 2001) for Bayesian analyses (MB), PAUP* v4.0 b10 (Swofford, 2002) for neighbour-joining (NJ) and maximum-parsimony (MP) analyses, and PhyML v2.4.4 (Guindon & Gascuel, 2003) for maximum-likelihood analyses (ML). Firstly, analyses were performed for 16S rRNA and COI separately, and secondly the incongruence length differences test (Mickevich & Farris, 1981; Farris *et al.*, 1994) was used to test phylogenetic congruence between the two analysed regions, and treated both genes together (homogeneity partition test in PAUP* v4.0 b10). The MP analyses were performed through a heuristic search with the tree bisection and reconnection (TBR) algorithm, with simple step-wise addition, and treating indels as a fifth state. The ML analyses were conducted in Phyml v2.4.4 using the model selected by ModelTest 3.7, and allowing the program to estimate the model parameters. Not all of the models from ModelTest 3.7 are implemented in PhyML v2.4.4; therefore, when the best-fitting model selected was not implemented, the second one was used in the ML analyses, as recommended by the authors.

We estimated support in different analyses by bootstrapping (Felsenstein, 1985): NJ (2000 pseudoreplicates), ML (500 pseudoreplications), and MP (1000 pseudoreplicates). For the Bayesian analyses, four chains were run for 5 000 000 generations, with a sample frequency of 100. Trees prior to the log likelihood stabilization tree were discarded as burn-in. The first 5000 trees were discarded in the analyses for the genera *Paramunida* and *Plesionida*, and the first 10 000 were discarded for the genera *Agononida* and *Munida*, such that 45 000 and 40 000 trees were computed for the consensus tree. Robustness of the inferred trees was evaluated through Bayesian posterior probabilities (BPPs).

RESULTS

SYSTEMATICS

AGONONIDA ISABELENSIS SP. NOV. (FIG. 1)

Material examined: Solomon Islands. SALOMON 1. Stn 1801, 09°25.0′S, 160°25.9′E, 1 October 2001, 254–271 m: 1 M, 20.7 mm (holotype, MNHN-Ga6496);

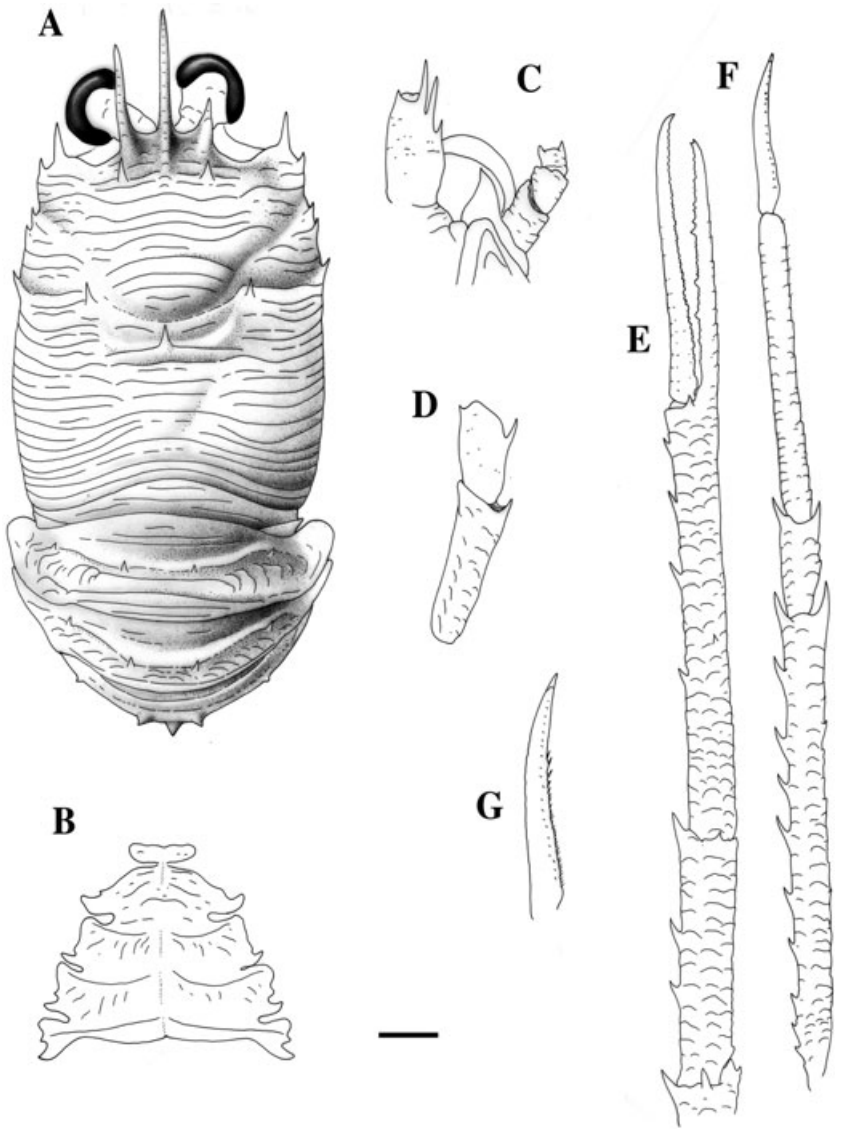

Figure 1. ***Agononida isabelensis*** **sp. nov.** male holotype, 20.7 mm (MNHN-Ga 6496), Solomon Islands. A, carapace and abdomen, dorsal view. B, sternum. C, left antennule and antenna, ventral view. D, ischium and merus of right third maxilliped, lateral view. E, right cheliped, lateral view. F, right P2, lateral view. G, dactylus, right P2, lateral view. Scale: A, B, E, F = 5 mm; C, D, G = 2 mm.

3 M, 14.0–20.7 mm; 3 ov. F, 17.2–18.4 mm (paratypes, MNHN-Ga6497). Stn 1802, 09°31.1′S, 160°35.0′E, 2 October 2001, 245–269 m: 2 M, 14.0–14.4 mm (paratypes, MNHN-Ga6498). Stn 1803, 09°32.1′S, 160°37.3′E, 2 October 2001, 308–347 m: 1 M 17.6 mm (paratype, MNHN-Ga6499). Stn 1860, 09°22′S, 160°31′E, 7 October 2001, 620 m: 5 M, 6.8–16.0 mm; 3 F, 7.2–14.4 mm (paratype, MNHN-Ga6500).

SALOMON 2. Stn 2210, 07°33.5′S, 157°42.3′E, 26 October 2004, 240–305 m: 11 M, 6.9–19.0 mm; 3 ov. F, 14.1–15.1 mm; 3 F, 9.4–11.5 mm (paratypes MNHN-Ga6501). Stn 2287, 8°39.84′S, 157°23.505′E, 6 November 2004, 253–255 m: 2 juv., 5.3–5.5 mm (paratypes, MNHN-Ga6502).

Etymology: From *Isabel*, one of the Solomon Islands from which some of the specimens were collected.

Description: Carapace as long as wide. Transverse ridges usually interrupted in cardiac and branchial regions by dense, short non-iridescent setae. Gastric region with two epigastric spines; one median cardiac spine and one postcervical spine on each side. Posterior border of carapace unarmed. Frontal margins transverse, slightly concave. Lateral margins slightly convex. Anterolateral spine strong at anterolateral angle, reaching or overreaching the level of the sinus between the rostrum and the supraocular spines. Second marginal spine before cervical groove 0.3 of

the preceding one. Branchial margins with three spines. Rostrum spiniform, nearly half as long as remaining carapace, straight, and horizontal. Supraocular spines (right spine regenerating in holotype) slightly thicker than rostral spine, clearly overreaching midlength of rostrum, and exceeding ends of corneas, slightly divergent, directed slightly upwards (Fig. 1A).

Thoracic sternites with numerous short striae. Anterior part of fourth sternite slightly narrower than third; median part of posterior margin of third sternite contiguous to fourth sternite. Transverse ridges between fifth, sixth, and seventh sternites obtuse, feebly granulated (Fig. 1B).

Second to fourth abdominal somites with four spines on anterior ridge, with some transverse striae and scales. Posterior ridge of fourth abdominal somite bears median spine.

Eyes large: maximum corneal diameter 0.3 times the distance between the bases of the anterolateral spines.

Basal segments of antennule (distal spines excluded) about 0.3 times the carapace length, elongate, overreaching corneae, with two distal spines, mesial spine clearly shorter than lateral spine; with two spines on lateral margin, proximal spine short, distal spine moderately long (Fig. 1C). First segment of antennal peduncle with stout process on mesial margin reaching end of second segment; second to fourth segments unarmed (Fig. 1C).

With Mxp 3 ischium about twice the length of the merus, measured along the dorsal margin, and distoventrally bearing a long spine. Merus with one well-developed median spine on flexor margin; extensor margin with small distal spine (Fig. 1D).

With P1s subequal in length, squamous, with some uniramous and plumose setae, and with some iridescent setae on mesial borders of merus and carpus, about five times the carapace length; merus clearly longer than carapace length, carpus four times longer than high, and 0.7 times palm length; palm nearly nine times longer than high, and 1.4 times longer than fingers. Merus armed with row of spines on mesial, ventral, and dorsal borders. Carpus and palm with row of spines on mesial margin, a few small spines on dorsal side. Fingers unarmed, with longitudinal carina on each side, distally curving and crossing, and ending in a sharp point (fixed finger of right cheliped in holotype regenerating) (Fig. 1E).

With P2 about three times the carapace length; merus nearly 1.5 times longer than carapace, between nine and ten times as long as high, 4.0–4.5 times the carpus length, and 1.3–1.5 times as long as propodus; propodus ten times as long as high, and nearly twice the dactylus length (Fig. 1F); end of propodus reaching or slightly overreaching end of P1 merus. Merus with spines along dorsal border, increasing in size distally, a few small spines along distal part of ventral margin, with distal spine strong. Carpus with strong distomesial and distoventral spine. Propodus with row of minute movable small ventral spinules (not discernible in Fig. 1F). Dactylus slightly curving distally, ventral margin slightly curving with 26–28 movable small spinules, distal third unarmed (Fig. 1F, G). Length, armature, and article proportions of P3 and P4 similar to those of P2.

Remarks: The new species closely resembles *Agononida prolixa* (Alcock, 1894) from the Arabian Sea, Sri Lanka, and the Andaman Sea (Ahyong & Poore, 2004; Baba, 2005). In both species, supraocular spines fall short of the rostral tip, the carapace has three branchial lateral spines, protogastric spines are absent, the fourth abdominal segment has one spine on the posterior transverse ridge, and the basal article of the antennal peduncle bears a moderately sized process, not overreaching the fourth article.

The two species may be distinguished as follows.

1. The posterior margin of the carapace is armed with two median spines in *A. prolixa*, whereas these spines are absent in the new species.
2. The distomesial angle of the second article of the antennal peduncle is armed with a spine in *A. prolixa*. In *A. isabelensis* sp. nov., this angle is unarmed.

The new species is also close to *Agononida similis* (Baba, 1988) from the Philippines and Indonesia (Baba, 1988). However, they can be differentiated according to the number of spines along the branchial margin of the carapace: four in *A. similis* and three in *A. isabelensis* sp. nov. Furthermore, the lateral margin of the basal article of the antennular peduncle has two well-developed spines in the new species, whereas this margin has only one spine in *A. similis*.

Distribution: Solomon Islands, at a depth of between 240 and 347 m.

MUNIDA CAELI SP. NOV. (FIG. 2)

Material examined: Solomon Islands. SALOMON 1. Stn 1801, 09°25.0′S, 160°25.9′E, 1 October 2001, 254–271 m: 1 M, 6.5 mm; 1 ov. F, 5.8 mm (paratype, MNHN-Ga6503). Stn 1802, 09°31.1′S, 160°35.0′E, 2 October 2001, 245–269 m: 1 M, 6.2 mm (paratype, MNHN-Ga6504); 1 ov. F, 6.0 mm (holotype, MNHN-Ga6505).

Etymology: The name *caeli* refers to one of the southern hemisphere constellations (the Graving Tool).

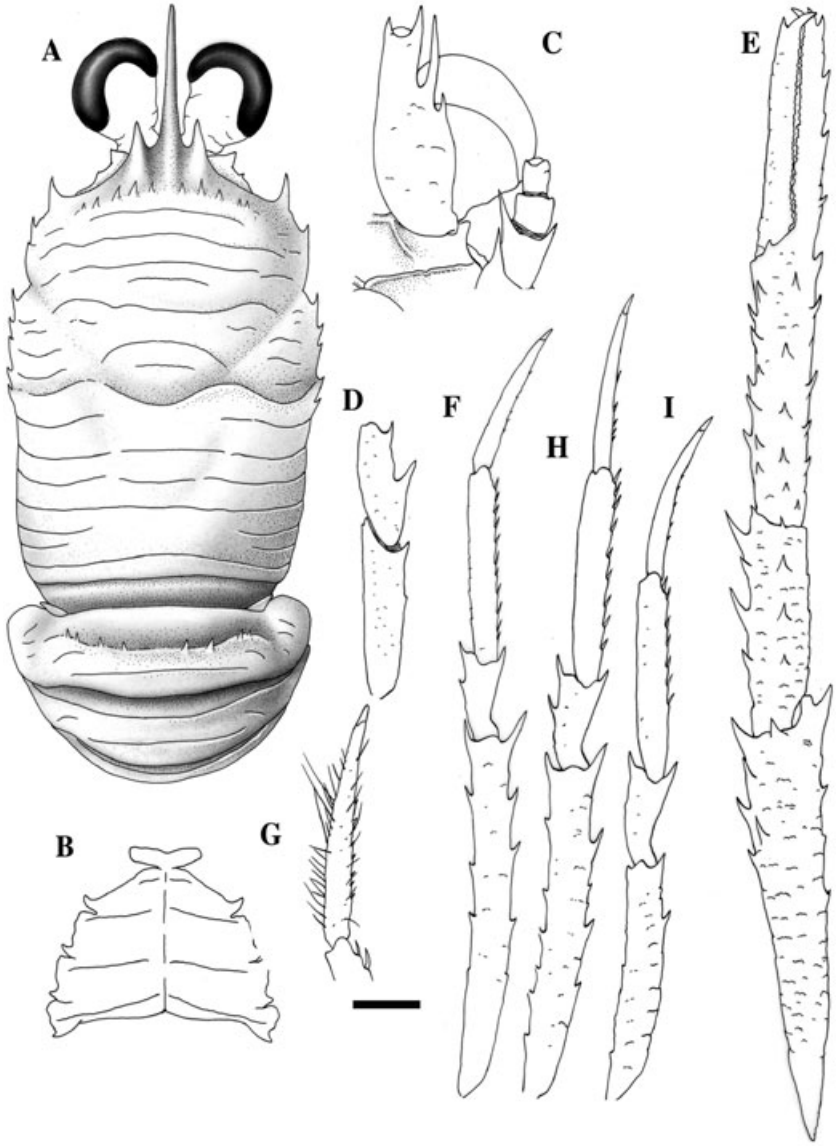

Figure 2. ***Munida caeli*** **sp. nov.**, ovigerous female holotype, 6.0 mm (MNHN Ga6505). Solomon Islands. A, carapace and abdomen, dorsal view. B, sternum. C, left antennule and antenna, ventral view. D, ischium and merus of right third maxilliped, lateral view. E, right cheliped, lateral view. F, right P2, lateral view. G, dactylus, right P2, lateral view. H, right P3, lateral view. I, right P4, lateral view. Scale: A, B, E, F, H, I = 1 mm; C, D, G = 0.5 mm.

Description: Carapace 1.2 times longer than wide, slightly convex dorsally. Transverse ridges mostly interrupted by dense short, non-iridescent setae. Intestinal region without striae or scales. Few scales, and secondary striae between main striae. Gastric region with a row of ten epigastric spines, other regions unarmed. Frontal margins slightly oblique. Lateral margins feebly convex. Anterolateral spine well-developed, situated at anterolateral angle, clearly not reaching the level of the sinus between the rostrum and the supraocular spines. Second marginal spine before cervical groove small, three times smaller than the preceding one. Branchial margins with five small spines, decreasing in size posteriorly. Rostrum spiniform, nearly half as long as remaining carapace, slightly curved. Supraocular spines short, not reaching midlength of rostrum, and clearly not exceeding ends of corneas, subparallel, upwardly directed (Fig. 2A).

Fourth thoracic sternite with a few small scales; lateral surface of fifth to seventh sternites smooth. Anterior part of fourth sternite narrower than third, slightly concave medially; median posterior margin of third sternite contiguous with fourth sternite.

Transverse ridges between fifth, sixth, and seventh sternites obtuse, feebly granulated (Fig. 2B).

Second abdominal tergite with eight spines on anterior ridge. Second and third tergites each with one transverse continuous stria.

Epistome crest without hump near mouth opening.

Eyes moderately large: maximum corneal diameter nearly half of the distance between the bases of the anterolateral spines.

Basal segment of antennule (distal spines excluded) about 0.25 times the carapace length, elongate, ending at the same level or slightly exceeding the corneas, with two distal spines, and with mesial spine shorter than lateral spine; two spines on lateral margin, proximal one short, located at midlength of segment, distal one long, nearly reaching end of distolateral spine (Fig. 2C). First segment of antennal peduncle with one distal spine on mesial margin, reaching end of second segment; second segment with two distal spines, mesial spine clearly longer than lateral spine, reaching end of third segment; third segment unarmed (Fig. 2C).

With Mxp 3 ischium nearly twice the length of the merus, measured along the dorsal margin, and distoventrally bearing a spine. Merus bearing two spines on flexor margin, proximal spine longer than distal spine; extensor margin unarmed (Fig. 2D).

With P1 squamate, three times the carapace length, with a few uniramous setae on the mesial borders of articles. Merus as long as carapace, nearly twice the carpus length, armed with some spines, and with stronger spines on distal border, not reaching proximal fourth of carpus. Carpus 3.5–4.5 times longer than high, shorter than hand, with a few strong spines on the mesial margin, and some short spines on the dorsal side. Palm as long as fingers, with row of spines along mesial and lateral borders, and some small spines on dorsal side. Fingers distally curving and crossing, and ending in a sharp point; fixed finger with some spines along entire border, with two distal spines, and ending in sharp point; movable finger unarmed, except for terminal spine (Fig. 2E).

With P2 twice the carapace length; merus slightly shorter than carapace, about 8–11 times as long as high, between four and five times the carpus length, and twice the propodus length; propodus between six and eight times as long as high, and 1.1–1.5 times longer than dactylus (Fig. 2F). Merus with row of some spines along dorsal and ventral borders. Carpus with several dorsal spines and one distoventral spine; end of carpus nearly reaching level of the merocarpal articulation of P1. Propodus with 9–12 movable ventral spinules. Dactylus long and slender, with dorsal margin slightly convex on proximal half, slightly curving distally with seven or eight movable spinules along ventral margin, distal third unarmed (Fig. 2G). P3 similar in length and armature to P2; P3 merus slightly shorter than P2 merus, and P3 propodus slightly longer than P2 propodus (Fig. 2H). P4 shorter than P2 and P3; P4 merus about 0.6 times P2 merus (Fig. 2I); merocarpal articulation reaching level of anterolateral spine of carapace.

Remarks: The new species resembles *Munida parca* Macpherson, 1996 from New Caledonia, and *Munida lailai* sp. nov. from Fiji (see below), in that it has five spines on the lateral margin of the carapace behind the cervical groove, eyes moderately large, the second abdominal segment with spines, lateral sections of the posterior thoracic sternites without granules, rostrum spiniform, the distomesial spine of the basal antennular segment clearly shorter than the distolateral spine, the distomesial spine of the second antennal article reaching the end of the third article, and with the distal half of the ventral border of the dactylus unarmed. The species can be easily distinguished from *M. parca* according to the following characters.

1. The antennular peduncle is longer in *M. parca* than in *M. caeli* sp. nov. The basal article is very long and clearly exceeds the corneae in *M. parca*, whereas this article only ends or slightly exceeds the corneae in the new species.
2. The distomesial spine of the second antennal segment exceeds the third segment in the new species, whereas this spine is shorter in *M. parca*, and falls short of the distal margin of the third segment.
3. The chelipeds (P1) are more elongate in the new species, with the carpus being 3.5–4.5 times longer than broad, whereas the carpus is twice as long as it is broad in *M. parca*.

Munida caeli sp. nov. is also closely related to *M. lailai* sp. nov. (see the differences under the Remarks section of *M. lailai* sp. nov.).

Distribution: Solomon Islands, at a depth of between 245 and 271 m.

MUNIDA LAILAI SP. NOV. (FIG. 3)

Munida parca Macpherson, 2004: 271.

Material examined: Fiji Islands. MUSORSTOM 10. Stn 1348, 17°30.29′S, 178°39.63′E, 11 August 1998, 353–390 m: 1 M, 5.9 mm (holotype, MNHN-Ga6506).

BORDAU 1. Stn 1450, 16°44.45′S, 179°58.50′E, 4 March 1999, 327–420 m: 1 F, 4.6 mm (paratype, MNHN-Ga6507).

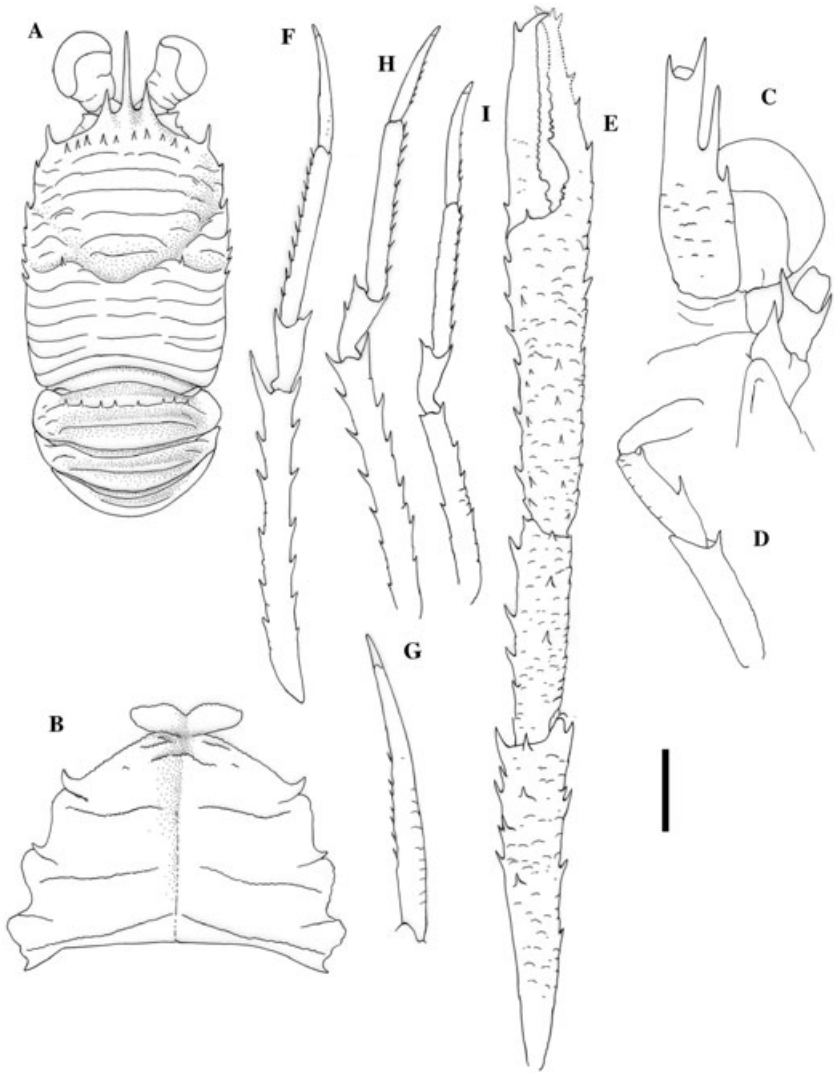

Figure 3. *Munida lailai* sp. nov., male holotype, 5.9 mm, (MNHN-Ga6506). Fiji Islands. A, carapace and abdomen, dorsal view. B, sternum. C, left antennule and antenna, ventral view. D, ischium and merus of right third maxilliped, lateral view. E, right cheliped, lateral view. F, left P2, lateral view. G, dactylus, left P2, lateral view. H, right P3, lateral view. I, right P4, lateral view. Scale: A, E, F, H, I = 2 mm; B, C, D, G = 1 mm.

Etymology: The name *lailai* means small in the Fijian language. The name may be considered as a noun in apposition.

Description: Carapace 1.2 times longer than wide. Transverse ridges usually interrupted in cardiac and branchial regions by very short, non-iridescent setae, and some scattered long iridescent setae. Intestinal region without scales. Dorsal surface of carapace armed with ten epigastric spines; one small postcervical spine on each side. Frontal margins slightly oblique. Lateral margins subparallel. Anterolateral spine well-developed, situated at anterolateral angle, clearly not reaching the level of the sinus between the rostrum and the supraocular spines. Second marginal spine before cervical groove small, about 0.25 times the length of the anterolateral spine. Branchial margins with five small spines. Rostrum spiniform, nearly 0.4 times the length of the remaining carapace, horizontal, carinated dorsally, and slightly convex. Supraocular spines short, not reaching midlength of rostrum, and clearly falling short of end of corneae, subparallel, slightly directed upwards (Fig. 3A).

Fourth thoracic sternite smooth, with a few short striae. Anterior section of fourth sternite narrower than third; median margin of third sternite contiguous with fourth sternite (Fig. 3B).

Second abdominal somite with eight spines along anterior ridge. Second and third somites each with one transverse stria.

Epistome crest without hump near mouth opening.

Eyes large: maximum corneal diameter 0.4 times the distance between the bases of the anterolateral spines.

Basal segment of antennule (distal spines excluded) about 0.4 times the carapace length, elongate, nearly three times longer than wide (excluding spines), overreaching end of corneae, with two distal spines, and with mesial spine clearly shorter than lateral spine; two spines on lateral margin, proximal one short, located at midlength of segment, distal one long, not reaching end of segment (excluding spines) (Fig. 3C). First segment of antennal peduncle with one short distomesial spine nearly reaching end of second segment; second segment with two distal spines, mesial spine slightly longer than lateral spine, not exceeding end of third segment; third segment unarmed (Fig. 3C).

With Mxp 3 ischium about 1.5 times the length of the merus, measured along the dorsal margin, and distoventrally bearing a spine. Merus of Mxp 3 with two well-developed spines on flexor margin, distal spine smaller; extensor margin unarmed (Fig. 3D).

With P1s subequal in length, about 4.5 times the carapace length, squamous, with numerous uniramous iridescent setae and plumose non-iridescent setae, denser on mesial and lateral borders of articles. Merus longer than carapace length, 1.5 times the carpus length, armed with some spines, with strongest spine on distal border, not reaching proximal fourth of carpus. Carpus four times as long as high, shorter than hand, several strong spines on mesial border, and some small spines on dorsal side. Palm 1.3 times longer than fingers, with row of mesial spines; some scattered small spines on dorsal side, and one row of lateral spines continuing onto fixed finger, and reaching tip. Movable finger unarmed, except proximal and distal spines. Fingers distally curving and crossing, ending in a sharp point, cutting edges slightly gaping in holotype (more straight in paratype), with small teeth of various sizes (Fig. 3E).

With P2 about three times the carapace length, with numerous uniramous iridescent setae and plumose non-iridescent setae along dorsal margins of articles; merus 1.3 times as long as carapace, about ten times as long as high, more than four times the carpus length, and 1.8 times as long as the propodus; propodus about nine times as long as high, and 1.3 times longer than dactylus (Fig. 3F). Dorsal border of merus with row of spines, increasing in size distally; ventral margin with row of spines, increasing in size distally. Carpus with distodorsal and distoventral spines; distal margin reaching the level of the merocarpal articulation of P1. Propodus with ten or 11 movable ventral spinules. Dactylus slightly curving distally, with seven movable spinules along ventral margin, and with distal third unarmed (Fig. 3G). P3 as long as P2; spination of P3 is similar to that of P2 (Fig. 3H). P4 length 0.8 times P2 length; merus 0.6 times the length of that of P2; spines along margins of merus and carpus less spinose than those of P2 and P3 (Fig. 3I); merocarpal articulation ending at the level of the anterolateral spine of the carapace.

Remarks: The new species is closely related to *M. parca* from New Caledonia (Macpherson, 1996) and *M. caeli* sp. nov. from the Solomon Islands (see above). The three species have five spines on the lateral margin of the carapace behind the cervical groove, eyes moderately large, the second abdominal segment with spines, the lateral portions of the posterior thoracic sternites without granules, rostrum spiniform, the epistome crest without a hump near the mouth opening, the distomesial spine of the basal antennular segment clearly shorter than the distolateral spine, and with the distomesial spine of the basal antennal article nearly reaching the end of the third article. *Munida lailai* sp. nov. can be distinguished from *M. parca* according to the following characters.

1. The chelipeds (P1) are clearly longer in the new species than in *M. parca*. In the new species, the length of P1 is about 4.5 times the carapace length, whereas this ratio is about 2.5 times in *M. parca*. The carpus is nearly 2.5 times longer than broad in *M. parca*, whereas it is four times longer than broad in the new species.
2. The walking legs (P2–P4) are longer in *M. parca*. P2 is about three times the carapace length in the new species, being slightly more than two times in *M. parca*. Furthermore, the merus of this leg is nearly as long as the carapace in *M. parca*, being longer in *M. lailai* sp. nov. In addition, the merocarpal articulation ends at the level of the anterolateral spine of the carapace in the new species, whereas in *M. parca* this articulation slightly exceeds the level of the anterior branch of the cervical groove.

On the other hand, *M. lailai* sp. nov. can be easily distinguished from *M. caeli* sp. nov. by the following aspects.

1. The antennular peduncle is clearly longer in *M. lailai* sp. nov. than in *M. caeli* sp. nov. The basal article clearly overreaches the corneae in *M. lailai* sp. nov., whereas this article only ends or slightly exceeds the corneae in *M. caeli* sp. nov.
2. The walking legs (P2–P4) are longer in *M. lailai* sp. nov. P2 is about three times the carapace length in *M. lailai* sp. nov., being twice the carapace length in *M. caeli* sp. nov.

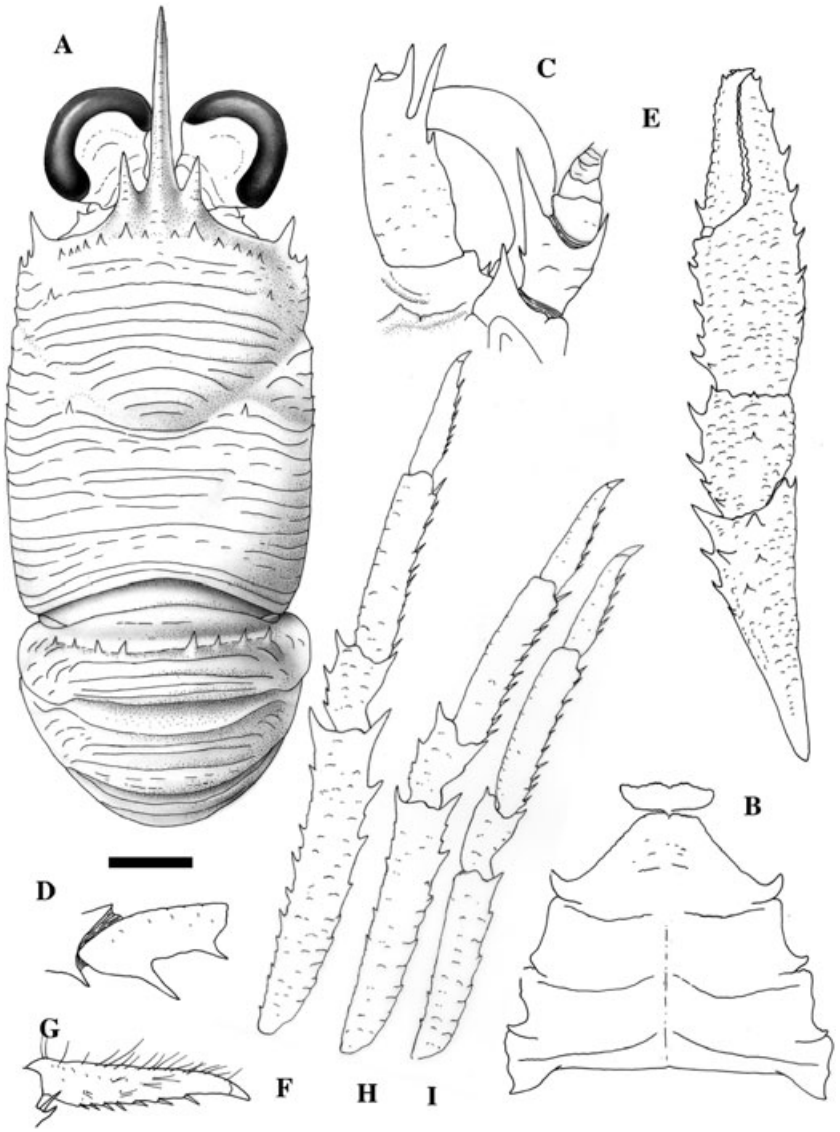

Figure 4. ***Munida mendagnai*** **sp. nov.**, male holotype, 7.3 mm (MNHN-Ga6510). Solomon Islands. A, carapace and abdomen, dorsal view. B, sternum. C, left antennule and antenna, ventral view. D, ischium and merus of right third maxilliped, lateral view. E, right cheliped, lateral view. F, right P2, lateral view. G, dactylus, right P2, lateral view. H, right P3, lateral view. I, right P4, lateral view. Scale: A, E, F, H, I = 1 mm; B, C, D, G = 0.5 mm.

Distribution: Fiji Islands, at a depth of between 327 and 420 m.

MUNIDA MENDAGNAI SP. NOV. (FIG. 4)

Material examined: Solomon Islands. SALOMON 1. Stn 1825, 09°50.5′S, 160°57.9′E, 4 October 2001, 340–391 m: 2 F, 7.1–7.2 mm (paratypes, MNHN-Ga6508). Stn 1826, 09°56.4′S, 161°03.9′E, 4 October 2004, 418–432 m: 1 M, 10.0 mm (paratype, MNHN-Ga6509); 1 M, 7.3 mm (holotype, MNHN-Ga6510).

Etymology: The name *mendagnai* is in honour of Alvaro de Mendaña, the Spanish explorer who named the Solomon Islands in 1568.

Description: Carapace 1.2 times longer than wide. Transverse ridges usually interrupted in cardiac and branchial regions by very short, non-iridescent setae, and by some scattered long iridescent setae. Small scales on intestinal region. Dorsal surface of carapace armed with 11–13 epigastric spines, one small hepatic, one parahepatic, and one postcervical spine on each side. Frontal margins transverse. Lateral margins subparallel. Anterolateral spine well-developed, situated at anterolateral angle, clearly not reaching the level of the sinus between the rostrum and the supraocular spines. Second marginal spine before cervical groove small, about 0.25 times the

length of the anterolateral spine. Branchial margins with five small spines. Rostrum spiniform, nearly 0.7 times the length of the remaining carapace, horizontal, dorsally carinated and slightly convex. Supraocular spines short, clearly not reaching the midlength of the rostrum, and not reaching the end of the corneae, subparallel, slightly directed upwards (Fig. 4A).

Fourth thoracic sternite smooth, with a few short striae. Anterior part of fourth sternite narrower than third; median margin of third sternite contiguous with fourth sternite (Fig. 4B).

Second abdominal somite with eight or nine spines along anterior ridge. Second and third somites each with between four and six transverse striae.

Epistome crest with hump near mouth opening.

Eyes large: maximum corneal diameter 0.5 times the distance between the bases of the anterolateral spines.

Basal segment of antennule (distal spines excluded) about 0.3 time the carapace length, elongate, about 2.5 times longer than wide (excluding spines), reaching end of corneae, with two distal spines, mesial spine shorter than lateral spine; two spines on lateral margin, proximal one short, located at midlength of segment, distal one long, reaching end of distal spines (Fig. 4C). First segment of antennal peduncle with one short distomesial spine nearly reaching the end of the second segment; second segment with two distal spines, mesial spine longer than lateral spine, slightly exceeding end of antennal peduncle, and with one additional mesial spine at midlength; third segment unarmed (Fig. 4C).

With Mxp 3 ischium about 1.5 times the length of the merus, measured along the dorsal margin, and distoventrally bearing a spine. Merus of Mxp 3 with two well-developed spines on flexor margin, distal margin smaller; extensor margin unarmed (Fig. 4D).

With P1s subequal in length, between 1.8 and 2.8 times the carapace length, squamous, with numerous uniramous iridescent setae and plumose non-iridescent setae, denser on mesial and lateral borders of articles. Merus shorter than carapace length, twice carpus length, armed with some spines, strongest spine on distal border, reaching proximal fourth of carpus. Carpus 1.4–1.7 times as long as high, shorter than hand, several strong spines on mesial border, and some small spines on dorsal side. Palm as long as fingers, with a row of mesial spines, with some scattered small spines on dorsal side, and one row of lateral spines continuing onto fixed finger and reaching tip. Movable finger unarmed, except proximal and distal spines. Fingers distally curving and crossing, ending in sharp points, cutting edges with small teeth of various sizes (Fig. 4E).

With P2 about twice the carapace length, with numerous uniramous iridescent setae and plumose non-iridescent setae along dorsal margins of articles; merus 0.8 times as long as carapace, between five and six times as long as high, 3.0–3.5 times the carpus length, and 1.5–1.8 times as long as the propodus; propodus between four and five times as long as high, and 1.2–1.3 times longer than dactylus (Fig. 4F). Dorsal border of merus with row of spines, increasing in size distally; ventral margin with row of spines, increasing in size distally. Carpus with several dorsal spines and one distoventral spine; distal margin clearly not reaching level of merocarpal articulation of P1. Propodus with between nine and 11 movable ventral spinules. Dactylus slightly curving distally, with seven movable spinules along ventral margin, distal fourth unarmed, ultimate spine clearly more remote from tip of dactylus than from penultimate spine (Fig. 4G). P3 0.9 times the length of P2; merus slightly shorter than that of P2; spination of P3 similar to that of P2 (Fig. 4H). P4 0.8 times the length of P2; merus 0.7 times the length of that of P2; spines along margins of merus and carpus less spinose than those of P2 and P3 (Fig. 4I); merocarpal articulation ending at the level of the anterior branch of the cervical groove.

Remarks: The new species is closely related to *Munida angusta* Macpherson, 2004 from the New Caledonia, Fiji, and Tonga islands (Macpherson, 2004). The two species have five spines on the lateral margin of the carapace behind the cervical groove, eyes large, the second abdominal segment with spines, lateral portions of the posterior thoracic sternites without granules, rostrum spiniform, the epistome crest with a hump near the mouth opening, the distomesial spine of the basal antennular segment clearly shorter than the distolateral spine, and the distomesial spine of the second antennal article reaching the end of the fourth article. The two species can be distinguished according to the following characters.

1. The second and third abdominal segments have between four and six transverse striae in the new species, instead of only one or two striae in *M. angusta*.
2. The chelipeds (P1) are clearly larger and shorter in the new species than in *M. angusta*. In the new species, the length of P1 is between 1.8 and 2.8 times the carapace length, whereas this ratio is between 3.0 and 4.5 times in *M. angusta*. The carpus is more than three times longer than broad in *M. angusta*, and 1.4–1.7 times longer than broad in the new species. The movable finger has a row of spines along the mesial margin in *M. angusta*, whereas this margin has only one proximal and one distal spine in the new species.

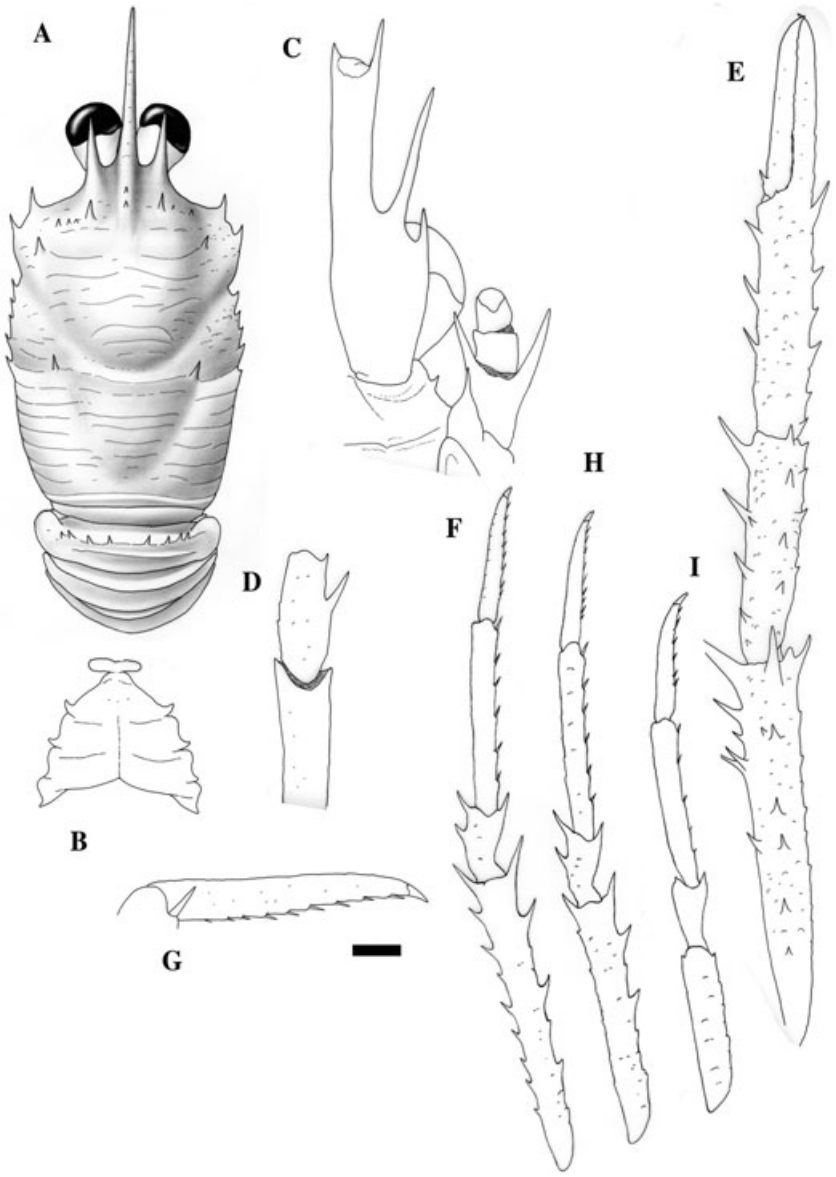

Figure 5. ***Munida oblongata*** **sp. nov.**, male holotype, 6.1 mm (MNHN-Ga6511). Solomon Islands. A, carapace and abdomen, dorsal view. B, sternum. C, left antennule and antenna, ventral view. D, ischium, and merus of right third maxilliped, lateral view. E, right cheliped, lateral view. F, right P2, lateral view. G, dactylus, right P2, lateral view. H, right P3, lateral view. I, right P4, lateral view. Scale: A, B, E, F, H, I = 1 mm; C, D, G = 0.5 mm.

3. The walking legs (P2–P4) are longer and more slender in *M. angusta*. P2 is about 1.5 times the carapace length in the new species, being 2.5 times that in *M. angusta*. Furthermore, the length of the merus of this leg is 0.8 times the carapace length in *M. mendagnai* sp. nov., being 1.2 times that in *M. angusta*. Finally, the dactyli of the walking legs are very slender, with the distal third of the ventral border unarmed in *M. angusta*, whereas dactyli are stouter, and the distal fourth of their ventral borders are unarmed, in the new species.

Distribution: Solomon Islands, at a depth of between 340 and 432 m.

MUNIDA OBLONGATA SP. NOV. (FIG. 5)

Material examined: Solomon Islands. SALOMON 2. Stn 2297, 9°05.69′S, 158°14.82′E, 8 November 2004, 728–777 m: 1 M, 6.1 mm (holotype, MNHN-Ga6511).

Etymology: From the Latin, *oblongus*, meaning longer than broad, referring to the long and slender basal segment of the antennule.

Description: Carapace 1.2 times longer than wide. A few secondary striae between main transverse ridges. Ridges with very short non-iridescent setae. Gastric region with one pair of well-developed and two pairs of small epigastric spines. Usually one parahepatic spine and one postcervical spine on each side. Frontal margins almost transverse. Lateral margins slightly convex. Anterolateral spine moderately long, near anterolateral angle, not reaching the level of the sinus between the rostrum and the supraocular spines. Second marginal spine before cervical groove smaller than preceding one. Branchial margins with five spines. Rostrum spiniform, about 0.6 times as long as remaining carapace, straight, and horizontal. Supraocular spines reaching midlength of rostrum, and not reaching end of corneae, subparallel, directed slightly upwards (Fig. 5A). Thoracic sternites smooth. Anterior margin of fourth sternite clearly narrower than third (Fig. 5B).

Second abdominal somite with row of eight spines on anterior ridge, with one transverse stria; third and fourth somites without stria.

Epistome crest without hump near mouth opening.

Eyes moderately large: maximum corneal diameter 0.3 times the distance between the bases of the anterolateral spines.

Basal segment of antennule (distal spines excluded) very long, nearly 0.5 times the carapace length, three times longer than wide (excluding spines), clearly overreaching end of corneae, with two distal spines, mesial spine shorter than lateral spine; two spines on lateral margin, proximal one short, located at midlength of segment, distal one long, not reaching end of distolateral spine (Fig. 5C). First segment of antennal peduncle with one moderately long distomesial spine nearly reaching end of second segment; second segment with two distal spines, mesial spine slightly smaller than lateral spine, exceeding third segment; third segment unarmed (Fig. 5C).

With Mxp 3 ischium about 1.5 times the length of the merus, measured along the dorsal margin, and bearing a spine distoventrally; merus with two spines on flexor margin, distal margin smaller; extensor margin unarmed (Fig. 5D).

With P1s subequal in length, about 2.5 times carapace length, squamous, with numerous non-iridescent uniramous and plumose setae, denser on mesial borders of articles. Carpus four times longer than high, as long as palm; palm slightly shorter than fingers. Merus armed with some spines, strongest spines on mesial and distal margins, reaching proximal quarter of carpus. Carpus with several spines along mesial, dorsal, and lateral sides. Palm with some spines along mesial and lateral margins, a few small spines on dorsal side. Fingers unarmed, except proximal spine on movable finger, distally curving and crossing, and ending in a sharp point (Fig. 5E).

With P2 about 2.4 times the carapace length; merus as long as the carapace, about 7.5 times as long as high, four times the carpus length and 1.6 times as long as propodus; propodus about seven times as long as high, 1.4 times dactylus length (Fig. 5F). Merus with well-developed spines along dorsal border, increasing in size distally, ventral margin with several spines and one long distal spine. Carpus with several dorsal spines, and one distoventral spine; distal margin clearly not reaching level of merocarpal articulation of P1. Propodus with six movable ventral spinules. Dactylus slightly curving distally, with eight movable spinules along entire ventral margin, last spinule very close to the end of the dactylus (Fig. 5G). P3 length 0.9 times P2 length, with similar spination and article proportions as in P2 (Fig. 5H). P4 length 0.8 times P2 length; merus nearly half the length of the P2 merus. Merus and carpus less spinose than those of P2 and P3 (Fig. 5I); merocarpal articulation ending at the level of the anterior branch of the cervical groove.

Remarks: Munida oblongata sp. nov. belongs to the group of species with five spines on the lateral margin of the carapace behind the cervical groove, eyes moderately large, the second abdominal segment with spines, the lateral parts of the posterior thoracic sternites without granules, rostrum spiniform, the epistome crest without a hump near the mouth opening, the basal article of the antennular segment very elongate, with the distomesial spine clearly shorter than the distolateral spine, the distomesial spine of the second antennal article not reaching the end of the fourth article, and with the distal half of the ventral border of the dactylus unarmed. The closest relative is *M. parca* from New Caledonia. The two species can be distinguished according to the following characters.

1. The supraocular spines reach the midlength of the rostrum in the new species, being clearly shorter in *M. parca*.
2. The basal segment of the antennular peduncle is three times longer than wide (excluding spines) in the new species, being less than 2.5 times that in *M. parca*.
3. The distal spines of the second segment of the antennal peduncle exceed the third segment in *M. oblongata* sp. nov., whereas these spines never reach the end of the third segment in *M. parca*.
4. The dorsal side of the P1 palm is armed with rows of spines in *M. parca*, whereas these spines are absent in the new species.
5. The movable spinules along the flexor margin of the dactylus of P2–P4 nearly reach the tip of the

article in the new species; this margin is unarmed in the distal third in *M. parca*. Furthermore, the dactyli are more curved in *M. parca* than in the new species.

On the other hand, *M. oblongata* sp. nov. can be easily distinguished from *M. caeli* sp. nov. and *M. lailai* sp. nov. by the following aspects.

1. The supraocular spines reach the midlength of the rostrum in *M. oblongata* sp. nov., being shorter in *M. caeli* sp. nov. and *M. lailai* sp. nov.
2. The basal segment of the antennular peduncle (excluding spines) is clearly longer in *M. oblongata* sp. nov. than in *M. caeli* sp. nov.
3. The distomesial spine of the second segment of the antennal peduncle overreaches the third segment in *M. oblongata* sp. nov., whereas in *M. lailai* sp. nov. the spine never reachs the end of the third segment, and in *M. caeli* sp. nov. the spine slightly exceeds it.
4. The dorsal side of the P1 palm is armed with rows of spines in *M. caeli* sp. nov. and *M. lailai* sp. nov., whereas these spines are absent in *M. oblongata* sp nov.
5. The movable spinules along the flexor margin of the dactylus of P2–P4 nearly reach the tip of the article in *M. oblongata* sp. nov. This margin lacks spinules in the terminal third in *M.caeli* sp. nov. and *M. lailai* sp. nov. Besides, the dactyli are more slender in *M. lailai* sp. nov. and *M. caeli* sp. nov. than in the new species.

Distribution: Solomon Islands, at a depth of between 728 and 777 m.

PARAMUNIDA LOPHIA SP. NOV. (FIG. 6)

Material examined: Solomon Islands. SALOMON 1. Stn 1831, 10°12.1′S, 161°19.2′E, 5 October 2001, 135–325 m: 1 M, 10.2 mm (holotype, MNHN-Ga6512); 2 M 13 mm (paratypes, MNHN-Ga6513). SALOMON 2. Stn 2191, 08°23.8′S, 159°27.1′E, 24 October 2004, 300 m: 1 ov. F, 10.2 mm (paratype, MNHN-Ga6514). Stn 2199, 7°43.3′S, 158°29.6′E, 25 October 2004, 296–304 m: 3 M, 9.1–11.8 m (paratypes, MNHN-Ga6515).

Etymology: From the Greek, *lophia*, for crest or ridge, referring to the longitudinal carina along the ventrolateral side of the second segment of the antennal peduncle. The name may be considered as a noun in apposition.

Description: Carapace as long as broad, excluding rostrum. Dorsal surface covered with minute spinules, with some scattered small spines and short uniramous setae. Gastric region distinctly separate from hepatic area, metagastric region well-defined; two small epigastric spines behind supraocular spines, and a median row of three well-developed spines, with the first thicker than the others. Cervical groove distinct. Cardiac region circumscribed, feebly convex, with a median row of three well-developed spines, and with the first thicker than the others. Anterior branchial region slightly separated from posterior branchial region. Frontal margin concave behind eye. Lateral margins convex, with some spines and iridescent setae on anterior half. Anterolateral spine short, reaching sinus between the rostral and the supraocular spines (Fig. 6A). Rostral spine spiniform, with thin, dorsal longitudinal carinae; supraocular spines well-developed and half as long as, and more slender than, rostrum (Fig. 6B). Lateral margins with some uniramous iridescent setae and some plumose non-iridescent setae.

Fourth thoracic sternite with few arcuate striae; fifth to seventh sternites smooth (Fig. 6C). Two median well-developed spines on anterior and posterior ridges of second and third abdominal somites. Fourth abdominal somite similar to preceding ones, but posterior ridge with distinct single median spine. Some small spiniform granules along anterior and posterior ridges of each somite.

Eye large: maximum corneal diameter about 0.3 times the distance between the bases of the external orbital spines.

Basal segments of antennule (distal spines excluded) overreaching corneae, with distomesial spine shorter than distolateral spine. First segment of antennal peduncle with anterior prolongation overreaching end of antennular peduncle, with long iridescent setae along mesial lateral margin. Second segment (spines excluded) about 1.5 times the length of the third segment, and 1.3 times longer than wide; distomesial spine long, mucronated, clearly exceeding antennal peduncle; distolateral spine not overreaching third segment. Ventral surface of second segment smooth, with a longitudinal carina along ventrolateral side; iridescent long setae along lateral side of distomesial spine continuing along ventrolateral crest. Third segment elongate, twice longer than wide and unarmed (Fig. 6D).

With Mxp 3 ischium about 1.5 times the length of the merus, measured along the dorsal margin, and bearing a spine distoventrally; merus with median, well-developed spine on flexor margin; extensor margin unarmed (Fig. 6E).

With P1 long and slender, between four and five times the carapace length, squamate, with some uniramous iridescent setae and some plumose non-iridescent setae, more dense along mesial margins. Mesial margins of merus, carpus, and palm with some small spines and acute scales. Carpus more than five

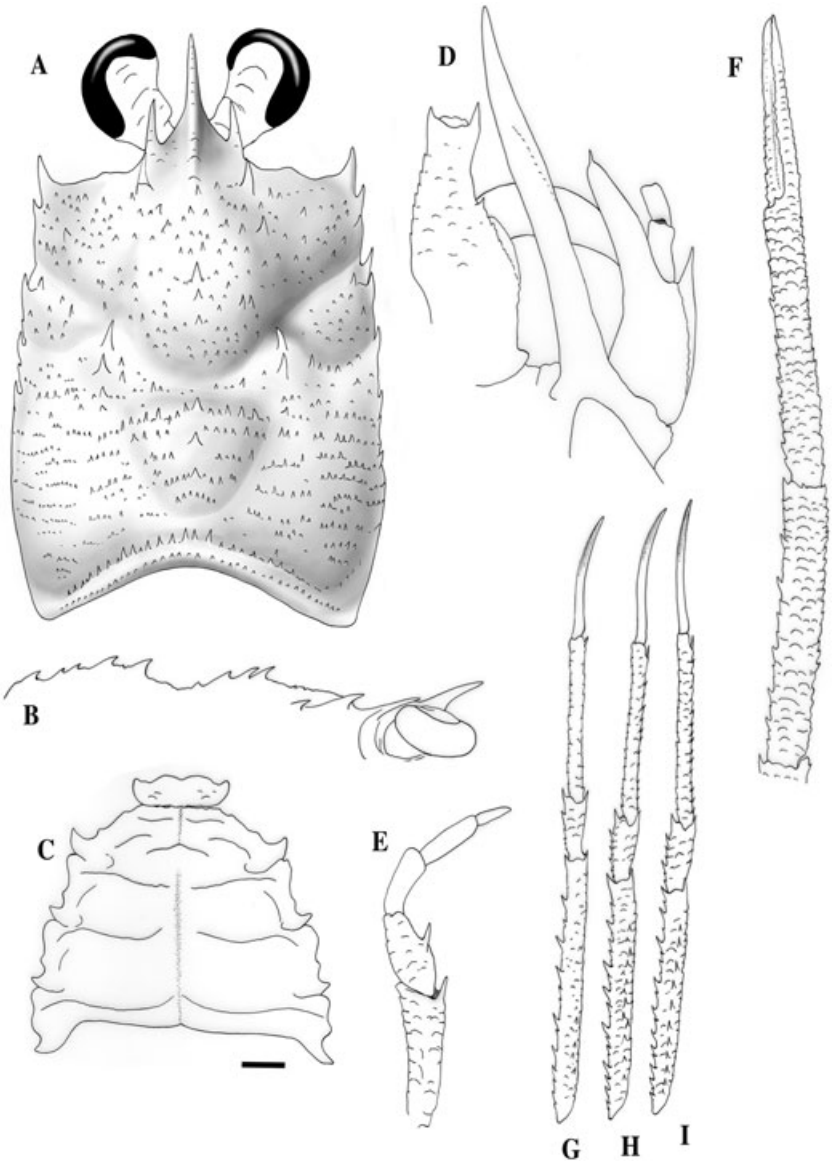

Figure 6. ***Paramunida lophia*** **sp. nov.**, male holotype, 10.2 mm (MNHN-Ga6512). Solomon Islands. A, carapace and abdomen, dorsal view. B, carapace, lateral view. C, sternum. D, left antennule and antenna, ventral view. E, right third maxilliped, lateral view. F, right cheliped, lateral view. G, right P2, lateral view. H, right P3, lateral view. I, right P4, lateral view. Scale: A, B, C = 1 mm; F, G, H, I = 2 mm ; D, E = 0.5 mm.

times longer than high. Palm as long as the carpus, and 1.4–1.5 times the length of the fingers (Fig. 6F).

With P2–P4 long and slender, subequal in length, with numerous scales on lateral sides of meri, carpi, and propodi; some uniramous iridescent setae and some plumose non-iridescent setae along dorsal and ventral borders. P2 about 3.5 times the carapace length; merus 1.5 times longer than carapace, about 10–11 times as long as high, 4.0–4.5 times as long as carpus and 1.4–1.7 times as long as propodus; propodus 9.5–10 times long as high, and 1.2–1.4 times the dactylus length (Fig. 6G). Merus with well-developed spines on dorsal border, increasing in size distally, ventral margin with a few spines, and one well-developed distal spine. Row of small spines along lateroventral margin. Carpus with some small dorsal spines; well-developed distal spine on dorsal and ventral margin. Propodus with small movable ventral spinules. Dactylus compressed, slightly curved, with longitudinal carinae along mesial and lateral sides, ventral border unarmed. End of P2 carpus nearly reaching end of P1 merus. P3 with similar spination and article proportions as P2. Merus slightly shorter than P2 merus; propodus and dactylus slightly longer

than those of P2 (Fig. 6H). P4 length 0.8–0.9 times the P2 length. Merus about 1.2–1.3 times the carapace length. Propodus and dactylus subequal to those of P3 (Fig. 6I). Merocarpal articulation falling short of anterior prolongation of first segment of antennal peduncle.

Remarks: The new species is close to *Paramunida salai* sp. nov. from the Solomon Islands (see below), and to *Paramunida belone* Macpherson, 1993 from New Caledonia, Futuna, Fiji, Tonga, and the Bali Sea (Macpherson, 1993, 2004; Baba, 2005). The three species are characterized by having a rostral spine that is larger than the supraocular spines, the thoracic sternites with a few arcuate striae, and the distomesial spine on the second antennal segment mucronated and reaching, or overreaching, the end of the fourth article.

The differences among the three species are provided in the Remarks section of *P. salai* sp. nov. (see below).

Distribution: Solomon Islands, at a depth of between 135 and 325 m.

PARAMUNIDA SALAI SP. NOV. (FIG. 7)

Material examined: Solomon Islands. SALOMON 1. Stn 1831, 10°12.1′S, 161°19.2′E, 5 October 2001, 135–325 m: 93 M, 6.4–11.5 mm; 49 ov. F, 8.2–10.7 mm (holotype ov. F, 8.6 mm, MNHN-Ga6517); 21 F, 6.7–8.8 mm (paratypes, MNHNGa-6516). Stn 1834, 10°12.2′S, 161°17.8′E, 5 October 2001, 225–281 m: 2 ov. F, 8.8–9.0 mm (paratypes, MNHN-Ga6518).

Etymology: This species name is dedicated to Enric Sala, for his contributions to marine conservation biology.

Description: Carapace nearly as long as broad, excluding rostrum. Dorsal surface covered with numerous spinules. Gastric region with two epigastric spines and a median row of three spines, with the first thicker than the others. Cervical groove distinct. Cardiac and anterior branchial regions slightly circumscribed. Cardiac region with a median row of three well-developed spines, with the first thicker than the others. Frontal margin slightly concave. Lateral margins convex, with some spines and iridescent setae on anterior half. Anterolateral spine short, clearly not reaching the sinus between the rostral and the supraocular spines (Fig. 7A). Rostral spine spiniform, with thin dorsal longitudinal carina; supraocular spines well-developed, and half as long as, and more slender than, rostrum (Fig. 7B).

Fourth thoracic sternite with a few arcuate striae, fifth to seventh nearly smooth, with one or two striae on each side (Fig. 7C).

Second and third abdominal somites each with two well-developed median spines on anterior and posterior ridge; ridges with numerous spinules and a few small spines. Fourth abdominal somite similar to preceding ones, but posterior ridge with distinct single median spine.

Eye large: maximum corneal diameter about 0.3 times the distance between the bases of the external orbital spines.

Basal segments of antennule (distal spines excluded) exceeding corneae, with distomesial spine small, and slightly shorter than distolateral spine (Fig. 7D). Anterior prolongation of first segment of antennal peduncle clearly overreaching antennular peduncle by about 0.25 of its length. Second segment (spines excluded) about twice the length of the third segment, and twice longer than wide, ventral surface without scales, with longitudinal carinae along ventrolateral margin; distomesial spine mucronated, reaching or slightly overreaching antennal peduncle, overreaching midlength of anterior prolongation of first article, although not reaching end of basal article of antennule (excluding distal spines), distolateral spine reaching or overreaching third segment, dorsomesial margin with longitudinal carina; third segment nearly twice longer than wide, and unarmed (Fig. 7D).

With Mxp 3 ischium about 1.5 times the length of the merus, measured along the dorsal margin, and bearing a spine distoventrally; merus with median well-developed spine on flexor margin; extensor margin unarmed (Fig. 7E).

With P1 long and slender, between 4.8 and 5.9 times the carapace length; carpus slightly longer than palm, and 5.5 times longer than high; palm of chelipeds nearly as long as fingers. Mesial margins of merus, carpus and palm with small spines and acute scales (Fig. 7F).

With P2–P4 long and slender, with numerous scales on lateral sides of meri, carpi, and propodi. P2 slightly shorter than P3, and longer than P4. P2 about 3.5 times the carapace length; merus 1.5 times longer than carapace, about 10–12 times as long as high, 4.5 times as long as carpus, and 1.4–1.6 times as long as propodus; propodus about ten times as long as high, and 1.2–1.4 times the dactylus length (Fig. 7G). Merus with well-developed spines on dorsal border, increasing in size distally, ventral margin with a few spines, and one well-developed distal spine; row of small spines along ventrolateral margin. Carpus with some small dorsal spines, well-developed distal spine on dorsal and ventral margin. Propodus with small movable ventral spinules. Dactylus compressed, slightly curved, with longitudinal carinae along mesial and lateral sides, ventral border unarmed. End of P2 carpus nearly reaching end of P1 merus. P3

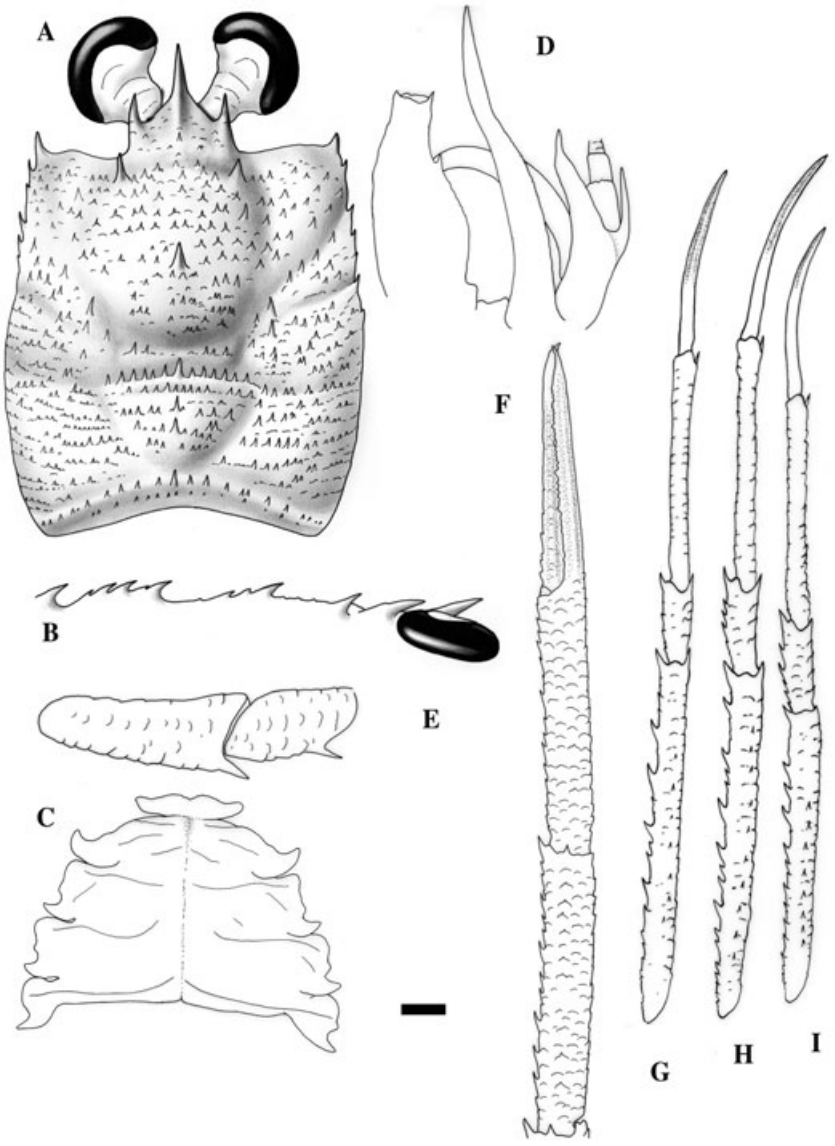

Figure 7. ***Paramunida salai*** **sp. nov.**, ovigerous female holotype, 8.6 mm (MNHN-Ga6517). Solomon Islands. A, carapace and abdomen, dorsal view. B, carapace, lateral view. C, sternum. D, left antennule and antenna, ventral view. E, right third maxilliped, lateral view. F, right cheliped, lateral view. G, right P2, lateral view. H, right P3, lateral view. I, right P4, lateral view. Scale: A, B, C = 1 mm; F, G, H, I = 2 mm; D, E = 0.5 mm.

with similar spination and article proportions as P2. Merus slightly shorter than P2 merus; propodus and dactylus slightly longer than those of P2 (Fig. 7H). P4 length 0.8–0.9 times P2 length. Merus about 1.2 times the carapace length. Propodus and dactylus slightly shorter than those of P3 (Fig. 7I). Merocarpal articulation slightly exceeding end of anterior prolongation of first segment of antennal peduncle.

Remarks: As mentioned above, *P. salai* sp. nov. is closely related to *P. belone* from New Caledonia, Futuna, Fiji, Tonga, and the Bali Sea (Macpherson, 1993, 2004; Baba, 2005), and *P. lophia* sp. nov. from the Solomon Islands. The three species can be distinguished from one another by several aspects.

Paramunida belone is easily differentiated from the two new species (*P. lophia* sp. nov. and *P. salai* sp. nov.) by the following characters.

1. The gastric region has only one median spine in *P. belone*, whereas this region has a median row of three spines, the first thicker than the others, in both *P. lophia* sp. nov. and *P. salai* sp. nov.
2. The walking legs (P2–P4) are longer in *P. belone* than in *P. lophia* sp. nov. and *P. salai* sp. nov. The

P2 merus is more than twice the carapace length in *P. belone*, and is about 1.5 times that in the two new species.

Furthermore, *P. salai* sp. nov. and *P. belone* can also be differentiated by the antennal peduncle. The distomesial spine of the second article of the antennal peduncle clearly exceeds the end of the antennal peduncle, and reaches or slightly overreaches the basal article of the antennular peduncle in *P. belone*; whereas this spine only slightly overreaches the end of the antennal peduncle, and clearly does not reach the end of the basal article of the antennular peduncle, in *P. salai* sp. nov.

The antennal peduncles are also different in *P. salai* sp. nov. and *P. lophia* sp. nov. The distomesial spine of the second segment clearly exceeds the antennal peduncle in *P. lophia* sp. nov., whereas it only reaches or slightly overreaches the antennal peduncle in *P. salai* sp. nov. Furthermore, the second segment (spines excluded) is about 1.5 times the length of the third segment, and is less than 1.5 times longer than wide in *P. lophia* sp. nov. This segment is twice the length of the third segment and twice longer than wide in *P. salai* sp. nov. Finally, the P1 palm is 1.4–1.5 times longer than the fingers in *P. lophia* sp. nov., whereas it is nearly as long as the fingers in *P. salai* sp. nov.

Distribution: Solomon Islands, at a depth of between 135 and 325 m.

PLESIONIDA CONCAVA SP. NOV. (FIG. 8)

Material examined: Solomon Islands. SALOMON 2. Stn 2260, 8°04.45′S, 156°55.87′E, 3 November 2004, 399–427 m: 4 M, 10.5–12.0 mm (holotype M, 12.0 mm; MNHN-Ga6520); 3 ov. F, 11.3–12.6 mm; 1 F, 7.7 mm (paratypes, MNHN-Ga6519).

Etymology: From the Latin *concavus*, meaning concave, referring to the concavity along the lateral side of the merus of the walking legs.

Description: Carapace as long as broad. Dorsal surface covered with numerous small spines. One epigastric spine, well-developed, behind each supraocular spine. Cardiac region slightly circumscribed. Frontal margins transverse. Rostrum 0.3 times the carapace length, compressed, slightly upturned, dorsally carinated, and not overreaching the cornea. Supraocular spines short, not reaching midlength of rostrum, and more slender than rostrum. Anterolateral spine large, reaching sinus between the rostral and the supraocular spines. Two or three small marginal spines before cervical groove. Branchial margins with four or five well- developed spines, and some small spinules. Posterior margin with numerous small spines (Fig. 8A).

Thoracic sternites smooth, without striae. Anterior part of fourth sternite narrower than third; median margin of third sternite contiguous with fourth sternite. Second to fourth abdominal somites with two transverse granulate ridges, lacking secondary transverse striae or scales; second somite without spines along anterior transverse ridge; third and fourth somites with two median spines on anterior ridge; one median spine on posterior ridge of fourth segment (Fig. 8B).

Eye large: maximum corneal diameter about 0.5 times the distance between the bases of the external orbital spines.

Basal segment of antennule (distal spines excluded) nearly reaching end of cornea, with distomesial spine shorter than distolateral spine; lateral border without spines. Anterior prolongation of first segment of antennal peduncle overreaching antennular peduncle; second segment with short distomesial spine, clearly not reaching end of third segment; third segment with small distomesial spine, clearly not reaching end of fourth segment. Second segment of antennal peduncle (spines excluded) about 1.5 times the length of the third segment, 1.5 times longer than wide; third segment as long as wide (Fig. 8C).

With Mxp 3 ischium slightly longer than the merus, and distoventrally bearing a spine. Merus with median well-developed spine on flexor margin; extensor margin unarmed (Fig. 8D).

With P1 subequal in length, between 2.5 and 3.0 times the carapace length, with a few setae; mesial margin of merus, carpus, and palm with spiniform crest, dorsal side with rows of small spines and some scattered granules. Merus shorter than carapace length, 1.5 times the length of the carpus, distomesial spine not reaching proximal fourth of carpus. Carpus 2.2–2.5 times as long as high, slightly shorter than hand. Palm slightly longer than fingers. Fingers with denticulated crest along mesial and lateral margins of movable and fixed finger, respectively, with longitudinal and rounded dorsal crest nearly reaching tips, distally curving and crossing, and ending in a sharp point; cutting edges with small teeth of various sizes (Fig. 8E).

With P2 about 2.5–2.7 times as long as carapace, with some iridescent uniramous setae, and numerous non-iridescent plumose setae, along dorsal margins of articles; merus slightly longer than carapace, about 4.5 times as long as high, nearly 3.5–4.0 times the carpus length, and 1.4–1.6 times as long as the propodus; propodus about 5.5–6.0 times as long as high, and 1.3–1.7 times longer than dactylus (Fig. 8F). Dorsal border of merus with row of spines, increasing

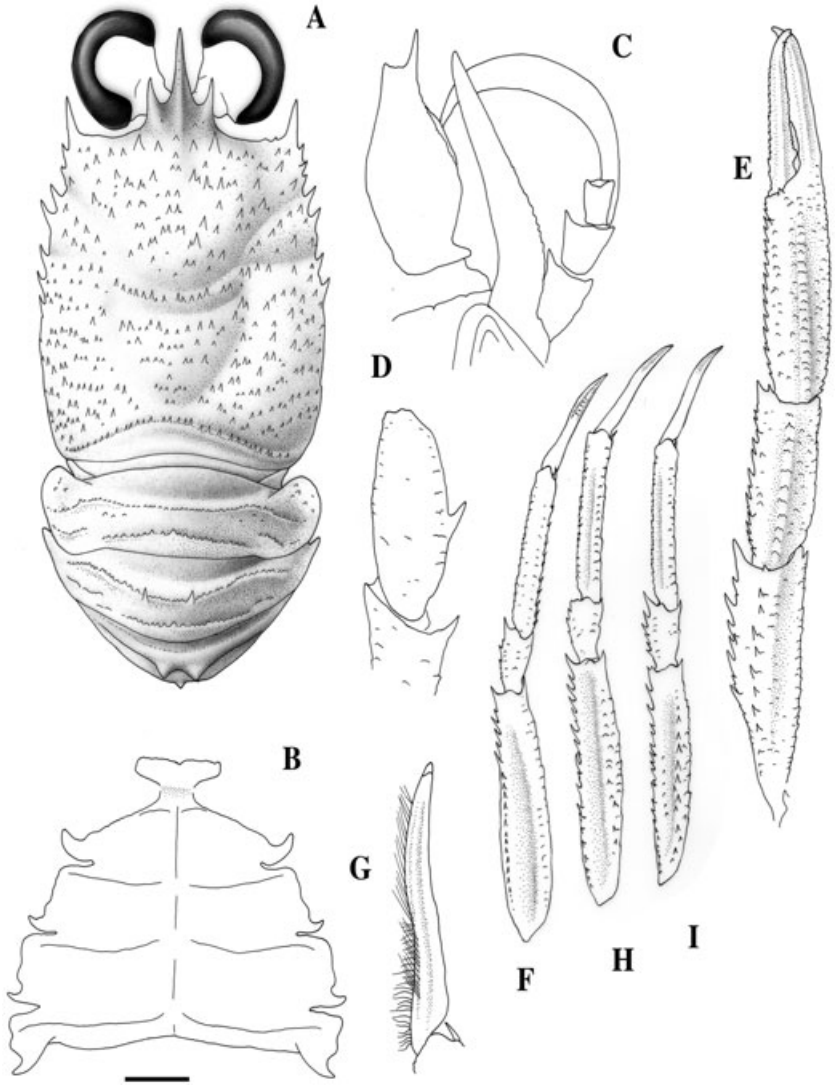

Figure 8. ***Plesionida concava*** **sp. nov.**, male holotype, 12.0 mm (MNHN-Ga6520). Solomon Islands. A, carapace and abdomen, dorsal view. B, sternum. C, left antennule and antenna, ventral view. D, ischium, and merus of right third maxilliped, lateral view. E, right cheliped, lateral view. F, right P2, lateral view. G, dactylus, right P2, lateral view. H, right P3, lateral view. I, right P4, lateral view. Scale: A, E, F, H, I = 2 mm; B, C, D, G = 1 mm.

in size distally, lateral side strongly concave; ventral border with row of short spines and well-developed distal spine. Carpus with some dorsal and ventral spines, increasing in size distally; distal margin slightly overreaching merocarpal articulation of P1. Propodus with 11–12 movable spinules along ventral margin, dorsal border serrated. Dactylus slightly curving, unarmed, dorsal border proximally slightly concave (Fig. 8G). P3 length slightly shorter than P2, with similar spination and proportions among articles (Fig. 8H). P4 length 0.9 times P2; merus 0.8–0.9 times the length of the P2 merus, lateral side less concave than in previous legs; ventral spines stronger than those of P2 and P3 meri (Fig. 8I). Merocarpal articulation ending at distal margin of corneae.

Remarks: The genus *Plesionida* Baba & de Saint Laurent, 1996, at present, contains two species: *Plesionida psila* Baba & de Saint Laurent, 1996, from the New Caledonia, and Wallis and Futuna islands (Baba, 2005; Macpherson & Baba, 2006), and *Plesionida aliena* (Macpherson, 1996), from New Caledonia, Fiji and Tonga (Baba, 2005). *Plesionida concava* sp. nov. is similar to *P. aliena* (Macpherson, 1996). However, they differ in the following features.

1. The carapace is covered by numerous small spines in the new species, whereas these spines are nearly absent in *P. aliena*, with only two epigastric spines and some granules, which are more numer-

ous and acute on the hepatic and branchial regions.
2. The P1s are more spiny in the new species than in *P. aliena*. In the new species, the mesial margin of the merus, carpus, and palm has a spiniform crest, and some spines scattered on the dorsal side of the articles. In *P. aliena*, the dorsal side of the articles is unarmed, and the mesial margin of the merus, carpus, and palm is serrated.
3. The lateral side of the merus of P2–P4 is concave in the new species and convex in *P. aliena*.

Distribution: Solomon Islands, at a depth of between 399 and 427 m.

Molecular analysis

Genus *Agononida*

After alignment with other sequences determined for the genus *Agononida* in a previous study (Machordom & Macpherson, 2004), 1187 bp were finally examined. The 16S rRNA sequence showed a high variability region between positions 245 and 272, which required the insertion of gaps. The partial COI sequence data set obtained consisted of 657 characters, of which 428 were constant, 29 were parsimony uninformative, and 200 were parsimony informative. For the 16S rRNA gene sequence, the resulting data set comprised 530 characters, of which 381 were constant, 22 were parsimony uninformative, and 127 were parsimony informative. Saturation tests indicated no saturation when we plotted all the substitutions together, but revealed saturation for transitions in the third codon positions of the COI gene for divergence values above 15%.

Intrageneric divergences between the new species and known species of the genus *Agononida* were in the range of 3.40–13.10% for 16S rRNA, and 8.70–17.88% for the COI gene. The new species showed the least divergence from *A. similis*: 3.40% for the 16S rRNA and 8.70% for the COI. The incongruence length difference (ILD) test revealed no significant incongruence among gene partitions ($P = 0.45$), and there were no strongly supported conflicting nodes among the tree topologies, so both genes were analysed in a combined data set, and only these results are presented.

The model that fitted the combined data set best was the GTR + I + Γ model (general time-reversible model; Lavane *et al.*, 1984; Rodríguez *et al.*, 1990), which gave an α-parameter of 1.3220 and an I-value of 0.5680. Base frequencies were A = 0.3220, C = 0.1480, G = 0.1739, and T = 0.3560, and the proportions of changes were 1.5688, 7.3481, 2.8003, 0.2082, and 16.2166. The selected outgroup was *Crosnierita dicata* (Macpherson, 1998), which was the closest genus to *Agononida* (Machordom & Macpherson, 2004). The species *Alainius crosnieri* Baba, 1991 was also included to test for a non-monophyletic origin of the genus. Relationships at terminal nodes were highly supported by bootstrap and posterior probability values (Fig. 9). At deep nodes, relationships were unresolved, and there was no support for the monophyly of the genus *Agononida*, but the new species in this genus was highly supported. Relationships among the different species exhibited a first cluster including *A. isabelensis* sp. nov. + *A. similis*, which was highly supported in all of the analyses. The sister group of this cluster was *Agononida procera* Ahyong and Poore, 2004, which was supported by all of the analyses. The species *Agononida marini* (Macpherson, 1994) appeared as a sister group of these three species, although support for this position was very low. The phylogenetic positions of the species *Agononida sphecia* (Macpherson, 1994) and *Agononida incerta* (Henderson, 1888) were not resolved.

Genera *Paramunida* and *Plesionida*

After alignment with other sequences of the genera *Paramunida* and *Plesionida*, determined in a previous study (Machordom & Macpherson, 2004), 1197 bp were finally analysed. The 16S rRNA sequence showed a high variability region between positions 245 and 272, requiring the insertion of gaps.

The partial COI sequence data set obtained for the two new species of the genus *Paramunida*, and for the new species of *Plesionida*, consisted of 657 characters, of which 437 were constant, 24 were parsimony uninformative, and 196 were parsimony informative. For the 16S rRNA gene sequence, the resulting data set comprised 540 characters, of which 398 were constant, 36 were parsimony uninformative, and 106 were parsimony informative. Saturation tests revealed no saturation for 16S rRNA and COI when we plotted all substitutions together. Intrageneric divergences within the *Paramunida* genus were in the range of 1.54–12.05% for the gene 16S rRNA, and of 2.95–17.35% for the COI. The lowest divergences for 16S rRNA were observed between *P. salai* sp. nov. and *P. belone*, and the lowest values for the COI sequences were detected between *P. salai* sp. nov. and *P. lophia* sp. nov.

For the genus *Plesionida*, the divergence between *P. aliena* and *P. concava* sp. nov. was 5.7% for 16S rRNA, and 10.85% for COI. The ILD test indicated no significant incongruence among gene partitions ($P = 0.48$), and there were no strong incongruences between the tree topologies, so both genes were analysed in a single matrix, and only the results of the combined data set are provided here.

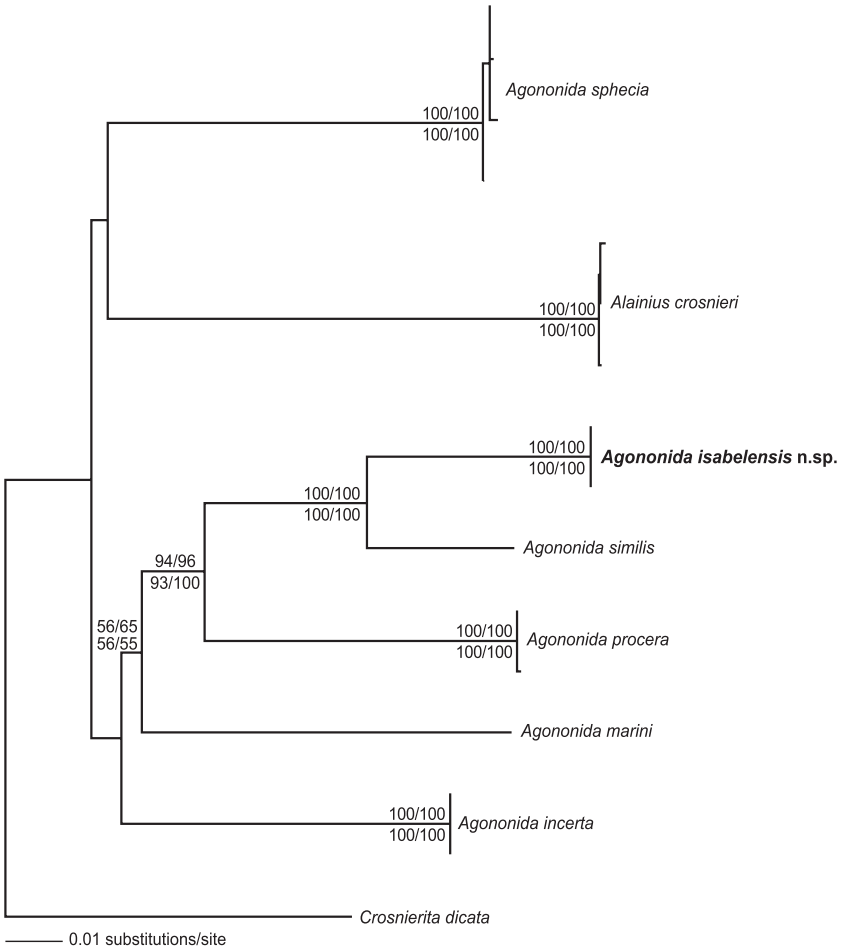

Figure 9. Neighbour-joining (NJ) tree based on the combined data set (16S rRNA and COI genes) showing phylogenetic relationships among *Agononida*. Numbers above branches indicate bootstrap values for the NJ and maximum parsimony (MP) analyses. Numbers below branches indicate bootstrap values for the maximum likelihood (ML) analyses and Bayesian posterior probabilities (BPPs).

The model that best fitted this combined data set was the GTR + I + Γ model (Lavane *et al.*, 1984; Rodríguez *et al.*, 1990), which gave an α-parameter of 1.4558 and an I-value of 0.6286. Base frequencies were A = 0.3234, C = 0.1371, G = 0.1664, and T = 0.3730, and the proportions of changes were 1.1171, 7.5925, 3.5999, 0.00001, and 17.8696.

The species *Onconida alaini* Baba & de Saint-Laurent, 1996 was selected as the outgroup, on the basis of previous results (Machordom & Macpherson, 2004) that showed the genus *Onconida* as the closest related genus to *Paramunida* and *Plesionida*. The monophyly of the genus *Paramunida* was highly supported by all of the tests (Fig. 10), although not all relationships within the genus were fully resolved. The phylogenetic relationship between the two new species *P. salai* sp. nov. and *P. lophia* sp. nov. was highly supported as a sister group, and these two species were in turn the sister group of the species *P. belone*.

The relationship between the species *Paramunida stichas* Macpherson, 1993 and *Paramunida proxima* (Henderson, 1885) was supported by all of the analyses. A comparison between samples of *P. stichas* from the Solomon Islands and from New Caledonia revealed two different groups separated by a mean divergence of around 1.1% for both genes (Fig. 10).

The last supported cluster included all of the species of the genus, except the species *Paramunida granulata* (Henderson, 1885), which always occupied a basal position. Relationships among the remaining species were not resolved.

Our analysis of two of the three species described for the genus *Plesionida* supported the monophyly of the group, with *P. aliena* as the sister group of *P. concava* sp. nov.

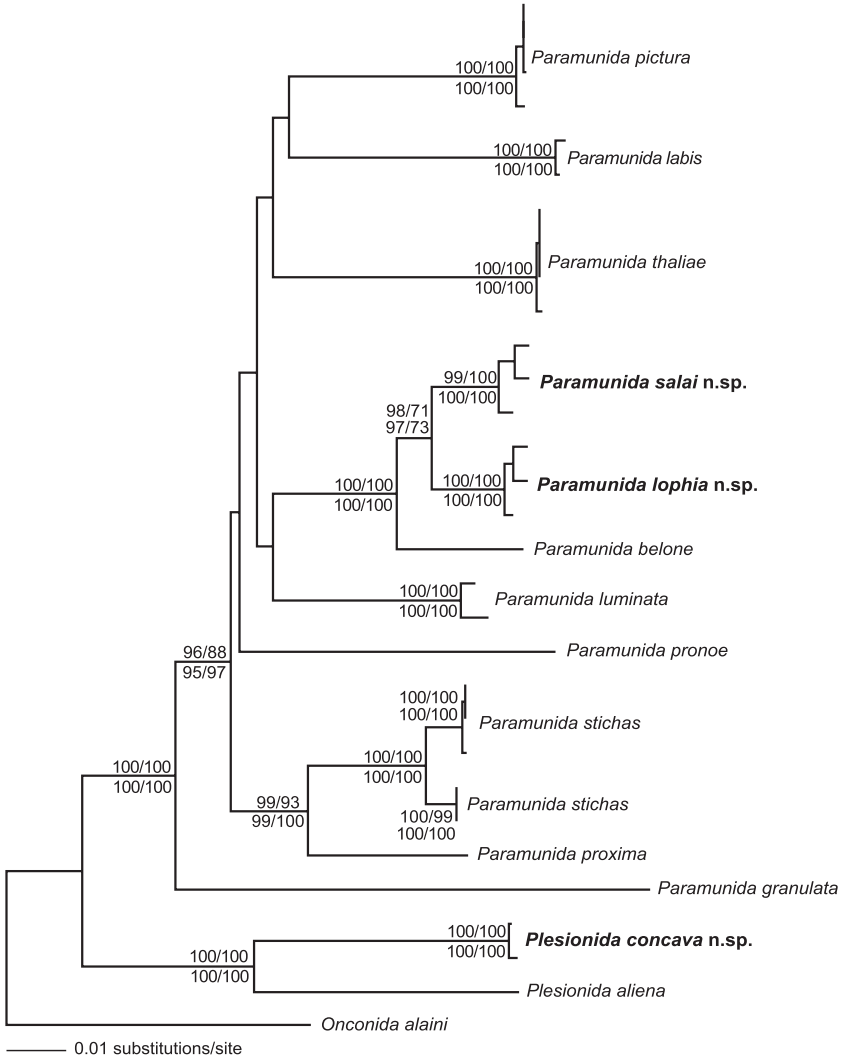

Figure 10. Neighbour-joining (NJ) tree based on the combined data set (16S rRNA and COI genes), showing phylogenetic relationships between *Paramunida* and *Plesionida*. Numbers above branches indicate bootstrap values for the NJ and maximum parsimony (MP) analyses. Numbers below branches indicate bootstrap values for the maximum likelihood (ML) analyses and Bayesian posterior probabilities (BPPs).

GENUS *MUNIDA*

After alignment with other sequences of the genus *Munida* determined in a previous study (Machordom & Macpherson, 2004; Macpherson & Machordom, 2005), 1199 bp were finally analysed. As for the other genera, the 16S rRNA gene showed a high variability region between positions 245 and 272 that required the insertion of gaps. The partial COI sequence data set obtained for the genus *Munida* consisted of 657 characters, of which 392 were constant, 19 were parsimony uninformative, and 246 were parsimony informative. For the 16S rRNA gene sequence, the resulting data set comprised 542 characters, of which 327 were constant, 50 were parsimony uninformative, and 165 were parsimony informative. Intrageneric divergence for the genus was in the range of 0.69–13.26% for the 16S rRNA gene, and of 3.50–20.24% for COI. The ILD test revealed no significant incongruence among the gene partitions ($P = 0.96$), and as for the other genera there were no incongruent topologies, so both genes were analysed in a single matrix. We also analyzed the 16S rRNA gene separately, as the COI gene could not be amplified in some species.

Tests for the 16S rRNA gene rendered no signs of saturation, but the COI gene sequence exhibited a certain level of saturation in transitions when all substitutions were plotted together, and also for third codon positions.

The model that best fitted the combined data set was the K81uf + I + Γ model (Kimura 3-parameters

model; Kimura, 1980), which gave an α-parameter of 0.5357 and an I-value of 0.5253. Base frequencies were A = 0.3893, C = 0.1068, G = 0.0969, and T = 0.4070, and the proportions of changes were 1.0000, 19.4012, 1.5268, 1.5268, and 19.4012. Model HKY + I + Γ (Hasegawa, Kishino & Yano, 1985) was selected for the ML analyses.

The model that best fitted the 16S rRNA data set was the TVM + I + Γ model (transversional model), which gave an α-parameter of 0.6255 and an I-value of 0.4306. Base frequencies were A = 0.3988, C = 0.0698, G = 0.1364, and T = 0.3950, and the proportions of changes were 1.2190, 19.2918, 2.6905, 0.0000, and 19.2918. Model GTR + I + Γ (Lavane *et al.*, 1984; Rodríguez *et al.*, 1990) was selected for the ML analyses.

The relationships of the genus *Munida* with other genera of the family remain unclear, therefore the species *Eumunida sternomaculata* de Saint Laurent and Macpherson, 1990 was selected as the outgroup, on the basis of previous studies (Morrison *et al.*, 2002; Machordom & Macpherson, 2004). Analysis of the combined data set (data not shown), and the 16S rRNA data set separately (Fig. 11), indicated two main clusters.

In the combined data set the basal cluster included the species *Munida delicata* Macpherson, 2004, and the type species of the genus *Munida rugosa* (Fabricius, 1775) from the North-East Atlantic, and the second cluster included the rest of the species of the genus. The basal group was supported in all of the analyses, with higher support in the Bayesian analyses than that indicated by the bootstrap. Divergences between these two species were quite high: 8.69% for the 16S rRNA gene and 15.80% for the COI gene. The second cluster was well supported except by the results of the Bayesian analysis.

As the COI gene sequence could not be amplified in the new species *M. oblongata* sp. nov., as in the species *Munida devestiva* Macpherson, 2006, the 16S rRNA gene sequence was analysed separately. In this analysis, these two species appeared in a basal cluster together with the species *M. rugosa* and *M. delicata* (Fig. 11). The type species *M. rugosa* was the sister lineage of the other three species, although bootstrap values and posterior probabilities were low. Divergence was in the range of 8.69–13.06%, which is high compared with that shown by the remaining species of the genus. The second cluster was divided into two different subgroups. All of the newly described species were included in the first subgroup. The species *M. lailai* sp. nov. appeared as the sister group of the species *M. parca* with high support. Divergence between these two species was low: 0.69% for the 16S rRNA gene and 4.75% for the COI gene. The species *M. caeli* sp. nov. was the sister lineage of these two species, also with high support, showing mean divergences of 1.87% (16S rRNA) and 7.45% (COI) from *M. parca*, and 1.64% and 8.11% from *M. lailai* sp. nov., respectively. The phylogenetic relationship of the species *M. mendagnai* sp. nov. was not fully resolved, although in all tree topologies it occupied a basal position in the first subgroup.

DISCUSSION

We described here eight new species of the family Galatheidae from the South-West Pacific, based on morphological and molecular data. We used molecular data to elucidate the phylogenetic relationships of the new species at the genus level.

Agononida

None of our analyses recovered the monophyly of the genus, in line with the results of a previous study (Machordom & Macpherson, 2004). In the present paper, we only inferred phylogenetic relationships among the newly described species and another five species of the genus. This results from the complexity of developing molecular analyses for the group, as we failed to amplify the COI gene for several species, making it difficult to establish relationships with a high level of confidence.

Despite this problem, our analyses were able to recover, with high support, the relationship between the new species, *A. isabelensis* sp. nov., and its sister group, *A. similis*, which is morphologically very similar. The two species can be easily differentiated according to the number of spines along the branchial margin of the carapace, and the number and size of spines on the basal article of the antennular peduncle, confirming the phylogenetic value of these characters. The relationship between this cluster and the species *A. procera* was also highly supported. The species *Alainius crosnieri* was also included in the analyses to check for the possibility of a polyphyletic origin of the group. Although all of the tree topologies located this species within the ingroup, this was not highly supported in any of the analyses. Further work is still required to clarify the apomorphic characters of the group, and its origin and diversification.

Paramunida and *Plesionida*

The genus *Paramunida* was identified with high support as a monophyletic group in all of the analyses, confirming the results of previous studies based on morphological and molecular characters (Baba, 1988; Machordom & Macpherson, 2004). The two new species described, *P. lophia* sp. nov. and *P. salai* sp. nov., were recovered as sister lineages, and showed

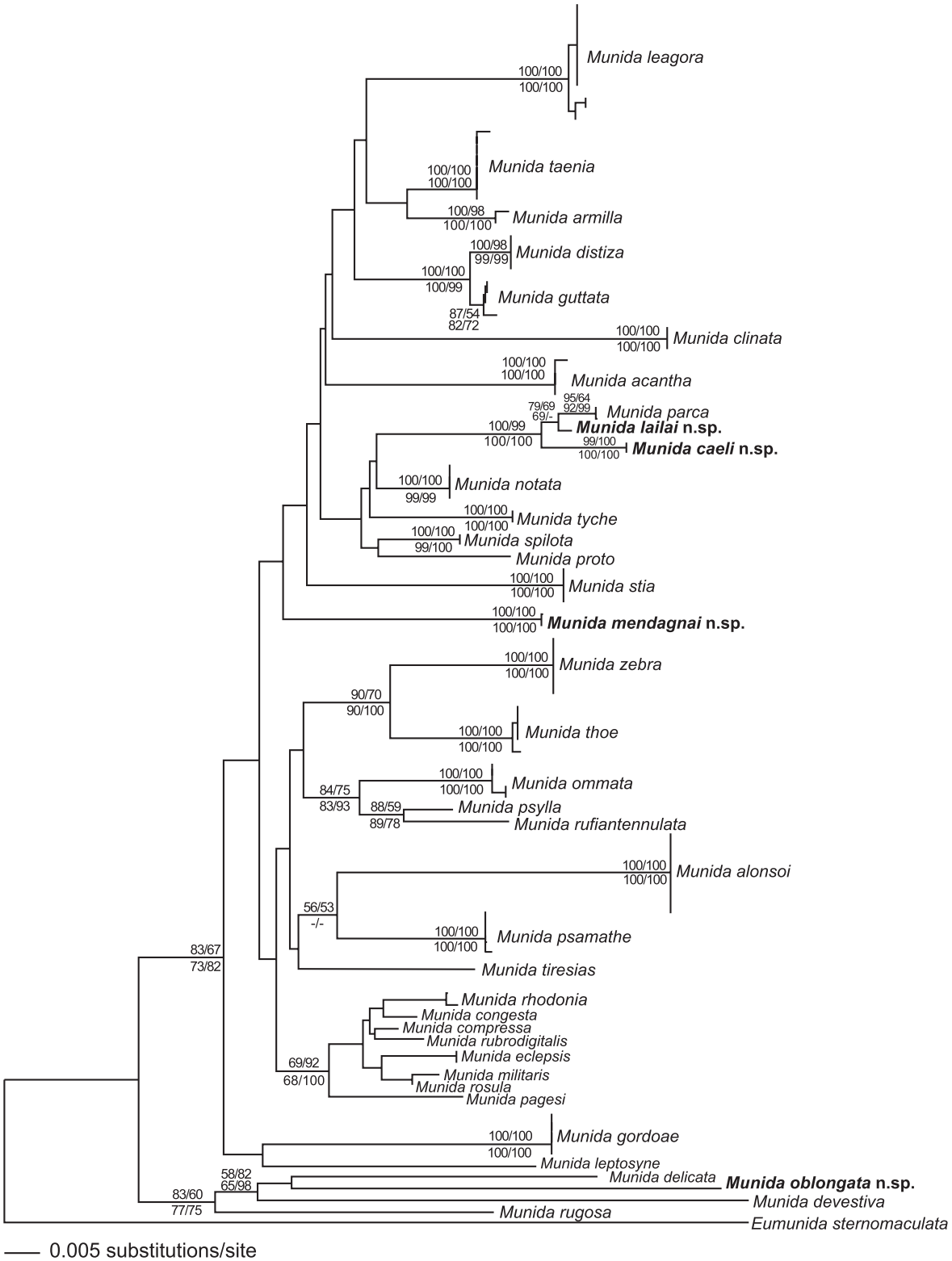

Figure 11. Neighbour-joining (NJ) tree based on the 16S rRNA data set showing phylogenetic relationships among *Munida*. Numbers above branches indicate bootstrap values for the NJ and maximum parsimony (MP) analyses. Numbers below branches indicate bootstrap values for the maximum likelihood (ML) analyses and Bayesian posterior probabilities (BPPs).

the lowest interspecific average divergence reported for the genus (1.9% for the 16S rRNA gene and 3.1% for the COI gene). Our morphological data support the taxonomic status of these two species, and diagnostic characters were constant in all specimens analysed. *Paramunida belone* appeared with high support as the sister group of the two new species, and also showed scarce divergence with respect to both species.

Low divergences seem to be a common pattern within this genus, with the exception of the species *P. granulata*. This last species is characterized by having a very long distomesial spine in the second article of the antennal peduncle, which is clearly shorter in the other species of the genus (Baba, 1988). This morphological difference, along with spinulation of the dorsal surface of the carapace, supports the divergence of *P. granulata* from the other species. In contrast, morphological differences between the two new species and *P. belone* were based on the shape of the antennal peduncle, suggesting that this appendix, as in *P. granulata*, is of phylogenetic value in the genus.

Specimens of the species *P. stichas* from the Solomon Islands were compared with others collected in the region of New Caledonia. These analyses differentiated the two areas, indicating a high mean intraspecific divergence of around 1.1% for both genes. The study of the mitochondrial gene ND1 (not included in this study) revealed the same tree topology, with a lower divergence value than the divergence indicated by the two genes analysed here (P. Cabezas, A. Machordom, E. Macpherson., unpubl. data).

Such low divergence values might be explained by a recent speciation event, or by speciation accompanied by slow morphological and molecular changes. This last scenario suggests a slow DNA substitution rate for this complex of species, a phenomenon that has been previously reported in other crabs and lobsters (Schubart *et al.*, 2001; Groeneveld *et al.*, 2007). A phylogeographic study of the genus in the Indo-West Pacific that is already underway, including morphological and molecular information, will help clarify the taxonomic position of *P. stichas* in the two regions, and the evolutionary history of the genus (P. Cabezas, A. Machordom, E. Macpherson., unpubl. data).

The genus *Plesionida* was analysed together with the genus *Paramunida* because only two of the three species described for the genus could be examined, and because previous studies (Machordom & Macpherson, 2004) have revealed that the genera are closely related. Our molecular analysis confirmed the taxonomic status of the genus, which had been inferred on the basis of morphological characters (Macpherson, 2004). *Plesionida concava* sp. nov. was compared with *P. aliena*, which is distributed in New Caledonia, Fiji, and Tonga. These two species were resolved with high support as a monophyletic group. A future analysis of the third species described for the genus will complete our knowledge of this group.

MUNIDA

The genus *Munida* is by far the most diverse taxon of the family Galatheidae, and is widely represented in the waters of the South-West Pacific. In an earlier study, we suggested the monophyly of the group in the area (Machordom & Macpherson, 2004), excluding the species *Munida callista* Macpherson, 1994, which was recently ascribed to a new genus (Cabezas *et al.*, 2008). The complexity of the group has previously been described in terms of extreme morphological convergence and heterogeneity in divergence values within species (Baba, 2005; Macpherson & Machordom, 2005).

The study of the combined data set and the separate 16S rRNA data set supported two differentiated clusters. The first cluster occupied a basal position, and included the type species *M. rugosa* from the North-East Atlantic and *M. delicata* from the Solomon Islands, whereas the species *M. oblongata* sp. nov. from the Solomon Islands and *M. devestiva* from New Caledonia were also included when we only considered the 16S rRNA data. Mean divergence values among the species were quite high (10.96% for 16S rRNA and 15.8% for the COI gene), but were within the range cited for other decapod taxa (Ptacek *et al.*, 2001; Harrison, 2004). For the COI gene, the value could be an underestimate because of saturation traces found in the third codon positions. For both genes, these values were higher than the mean divergence reported for the genus (Machordom & Macpherson, 2004), and similar divergence values have been found in species such as *Enriquea leviantennata* (Baba, 1988) and *Babamunida callista* (Macpherson, 1994), which were excluded from the genus *Munida* on the basis of morphological and molecular information.

Additionally, the new species *M. oblongata* sp. nov. is morphologically very close to the species *M. parca* from New Caledonia, although genetically they show a deep divergence. Although this pattern seems to be common in decapods (Knowlton, 1986), additional explanations are also possible. The undersampling of more closely related taxa might lead to the same pattern. A future increase of the sampling effort is essential to evaluate the overall diversity of galatheids in the area. And extinction events in the group could be an alternative explanation, although with our data it is not possible to confirm this hypothesis.

The second cluster included the rest of the species of the genus, all from the South-West Pacific. Three new species of the genus *Munida* appeared in this cluster. Although most relationships at the internal nodes were unresolved, *M. lailai* sp. nov. was highly supported as a sister group of the species *M. parca*, and these two species were supported as a sister lineage to *M. caeli* sp. nov. Divergence values between these two species were very low, although they were similar to divergences reported for other species complexes such as *Munida militaris* Henderson, 1885 + *Munida rosula* Macpherson, 1994 + *Munida compressa* Baba, 1988 (Machordom & Macpherson, 2004). Morphologically, the two new species resemble *M. parca*, and although morphological differences are subtle, these were constant in all of the specimens examined. The phylogenetic position of the species *M. mendagnai* sp. nov. was not resolved, but it appeared in the second cluster with *M. caeli* sp. nov. and *M. lailai* sp. nov. in all the analyses. All three new species included in this cluster showed a low genetic divergence, with a very similar morphology.

This marked difference between the first and the second cluster was emphasized in a previous study (Cabezas *et al.*, 2008), in which *M. rugosa* was not included in the ingroup of the genus *Munida*, and showed a clear genetic difference with respect to the rest of species of the genus. Morphologically, there are no apparent characters to differentiate species from both clusters, although differences in epistome shape and armature, as have been observed between *Munida* and *Babamunida* (Cabezas *et al.*, 2008), as well as antenna and antennula insertions, should be considered. On the other hand, the heterogeneity observed in the divergence values could indicate that different radiation events have shaped the diversification of the genus.

All of this information emphasizes the need for further more detailed analyses of more species from the Indo-Pacific and Atlantic-Mediterranean oceans, as well as the study of more conserved genes, to clarify the taxonomy of this group of species.

Evolutionary considerations

The taxonomic status of the new species was supported by both morphological and molecular data, although intrageneric relationships could not be deduced with confidence for all of the species. This low resolution seems to be the general pattern for the family Galatheidae, and has already been noted in other studies in which relationships at the genus level were also unresolved (Machordom & Macpherson, 2004). This conspicuous feature might be related to a scenario resulting from a rapid speciation process, rather than from a lack of resolution or paucity of the molecular markers used. The number of informative positions and the low levels of saturation indicate that both genes are appropriate for the study of this group. In addition, previous works have described the mitochondrial genes 16S rRNA and COI as powerful tools to elucidate phylogenetic relationships in crustacean decapods (Porter, Pérez-Losada & Crandall, 2005), and in other marine groups (e.g. sponges; Blanquer & Uriz, 2007). Our phylogenies displayed a large number of short internal branches relative to long terminal branches. However, some groups of species also showed short terminal branches, which suggest recent speciation events.

Although the data did not show a clear geographic structure, New Caledonia seems to be the ancestral area for the different genera, although a deeper phylogeographic study is necessary to test this fact.

These results suggest an evolutionary history shaped by rapid diversification and radiation events, probably related to the marine and geological complexity of the area (Holloway & Hall, 1998).

Events of rapid diversification are common within Crustacea, including decapods (Schram, Feldmann & Copeland, 1978), making it difficult to resolve relationships at ancient nodes, and to thus estimate divergence times. The Eocene (Schram, 1986) has been proposed as the scene for extensive decapod radiation, and Machordom & Macpherson (2004) located the diversification of the genus *Munida* in the Late Miocene, using two mitochondrial genes. An older estimation has been suggested by Porter *et al.* (2005), dating the diversification of Anomuran crabs (including the Galatheidae family) in the Permian–Triassic, using a multi-locus estimation procedure based on nuclear and mitochondrial genes. It is clear that the use of mitochondrial markers alone is insufficient for resolving such ancient speciation processes, as the substitution rate leads to a high probability of homoplasy. Thus, further investigations, including additional morphological and molecular characters, are still required to understand the evolutionary history of the group.

Previous studies have demonstrated the usefulness of nuclear genes to resolve phylogenetic relationships at high taxonomic levels (Tudge & Cunningham, 2002; Ahyong *et al.*, 2007). Morphologically, the extreme convergence observed in this family makes it very difficult to find new morphological characters of phylogenetic value, and the most common morphological characters used in the traditional taxonomy of the family show a high degree of homoplasy. Nevertheless, characters not previously considered, such as those describing the epistome region, can provide new synapomorphies (Cabezas *et al.*, 2008). If combined with additional genes with lower substitution rates,

such as conserved genes, these characters could improve the resolution obtained at the basal nodes of the phylogenies.

ACKNOWLEDGEMENTS

The authors thank A. Crosnier and B. Richer de Forges for providing the material needed for this study, the authors of PhyML for their help with the program, and Regina Cunha for assistance with data analysis. We are also very grateful to Fernando Alda for his help and valuable comments on the manuscript, and Lourdes Alcaraz for technical assistance in the lab. We also thank Kareen Schnabel and an anonymus rewiever for their suggestions to improve the manuscript. Finally, we are indebted to Deborah Bailie for providing the *Munida rugosa* sequence of the 16S rRNA gene, and to A. Burton for revising the English. This study was funded by MEC project CTM2004-01769. PC was supported by a grant from the Consejo Superior de Investigaciones Científicas (CSIC).

REFERENCES

Ahyong ST. 2007. Decapod Crustacea collected by the NORFANZ expedition: Galatheidae and *Polychelidae*. *Zootaxa* **1593:** 1–54.

Ahyong ST, Galil BS. 2006. Polychelidae from the southern and western Pacific (Decapoda, Polychelida). *Zoosystema* **28:** 757–767.

Ahyong ST, Lai JCY, Sharkey D, Colgan DJ, Ng PKL. 2007. Phylogenetics of the brachyuran crabs (Crustacea: Decapoda): The status of Podotremata based on small subunit nuclear ribosomal RNA. *Molecular Phylogenetics and Evolution* **45:** 576–586.

Ahyong ST, Poore GCB. 2004. Deep-water Galatheidae (Crustacea: Decapoda: Anomura) from southern and eastern Australia. *Zootaxa* **472:** 3–76.

Akaike H. 1974. New look at statistical model identification. *IEEE Transactions on Automatic Control* **19:** 716–723.

Baba K. 1988. Chirostylid and galatheid crustaceans (Decapoda: Anomura) of the 'Albatross' Philippine Expedition, 1907–1910. *Researches on Crustacea, Special Number* **2:** 1–203.

Baba K. 1995. A new squat lobster (Decapoda: Anomura: Galatheidae) from an active thermal vent area in the North Fiji Basin, SW Pacific. *Crustacean Research* **24:** 188–193.

Baba K. 2005. Deep-sea chirostylid and galatheid crustaceans (Decapoda: Anomura) from the Indo-West Pacific, with a list of species. *Galathea Reports* **20:** 1–317.

Baba K, de Saint Laurent M. 1996. Crustacea Decapoda: revision of the genus *Bathymunida* Balss, 1914, and description of six new related genera (Galatheidae). In: Crosnier A, ed. *Résultats des Campagnes MUSORSTOM*, Vol. 15. *Mémoires du Muséum National d'Histoire Naturelle* **168:** 433–502.

Blaber SJM, Milton DA. 1990. Species composition, community structure and zoogeography of fishes of mangrove estuaries in the Solomon Islands. *Marine Biology* **105:** 259–267.

Blanquer A, Uriz MJ. 2007. Cryptic speciation in marine sponges evidenced by mitochondrial and nuclear genes: a phylogenetic approach. *Molecular Phylogenetics and Evolution* **45:** 392–397.

Bruce AJ. 1980. Some Pontoniine shrimps from the Solomon Islands. *Micronesia* **16:** 261–269.

Cabezas P, Macpherson E, Machordom A. 2008. A new genus of squat lobster (Decapoda: Anomura: Galatheidae) from the South West Pacific and Indian Ocean inferred from morphological and molecular evidence. *Journal of Crustacean Biology* **28:** 68–75.

Castro P. 2005. Crabs of the subfamily Ethusinae Guinot, 1977 (Crustacea, Decapoda, Brachyura, Dorippidae) of the Indo-West Pacific region. *Zoosystema* **27:** 499–600.

Challis DA. 1969. An ecological account of marine interstitial opisthobranchs of British Solomon Islands Protectorate. *Philosophical Transactions of the Royal Society of London Series B-Biological Sciences* **255:** 527–539.

Cleva R, Crosnier A. 2006. Heterocarpus tenuidentatus, a new species of shrimp from the Solomon Islands (Crustacea, Decapoda, Caridea, Pandalidae). *Zootaxa* **1200:** 61–68.

Cubelio SS, Tsuchida S, Hendrickx ME, Kado R, Watanabe S. 2007. A new species of vent associated Munidopsis (Crustacea: Decapoda: Anomura: Galatheidae) from the Western Pacific, with notes on its genetic identification. *Zootaxa* **1435:** 25–36.

Farris JS, Kallersjo M, Kluge AG, Bult C. 1994. Testing significance of incongruence. *Cladistics. The International Journal of the Willi Hennig Society* **10:** 315–319.

Felsenstein J. 1985. Confidence limits on phylogenies: an approach using the bootstrap. *Evolution* **39:** 783–791.

Folmer O, Black M, Hoeh W, Lutz R, Vrijenhoek R. 1994. DNA primers for amplification of mitochondrial cytochrome c oxidase subunit I from diverse metazoan invertebrates. *Molecular Marine Biology and Biotechnology* **3:** 294–299.

Galil BS. 2007. The deep-water Calappidae, Matutidae and Leucosiidae of the Solomon Islands, with a description of a new species of *Euclosia* Galil, 2003 (Crustacea, Decapoda, Brachyura). *Zoosystema* **29:** 555–563.

Goggin L. 2004. Solomon Islands: a marine life survey. *Tropical Conservancy* **5:** 8–11.

Groeneveld JC, Gopal K, George RW, Matthee CA. 2007. Molecular phylogeny of the spiny lobster genus *Palinurus* (Decapoda: Palinuridae) with hypotheses on speciation in the NE Atlantic/Mediterranean and SW Indian Ocean. *Molecular Phylogenetics and Evolution* **45:** 102–110.

Guindon S, Gascuel O. 2003. A simple, fast, and accurate algorithm to estimate large phylogenies by maximum likelihood. *Systematic Biology* **52:** 696–704.

Harrison JS. 2004. Evolution, biogeography, and the utility of mitochondrial 16S and COI genes in phylogenetic analysis of the crab genus *Austinixa* (Decapoda: Pinnotheridae). *Molecular Phylogenetics and Evolution* **30:** 743–754.

Hasegawa M, Kishino H, Yano TA. 1985. Dating of the

human ape splitting by a molecular clock of mitochondrial DNA. *Journal of Molecular Evolution* **22:** 160–174.

Holloway JD, Hall R. 1998. SE Asian geology and biogeography: an introduction. In: Hall R, Holloway JD, eds. *Biogeography and geological evolution of SE Asia*. Leiden: Backhuys Publishers, 1–23.

Huelsenbeck JP, Ronquist F. 2001. MRBAYES: Bayesian inference of phylogenetic trees. *Bioinformatics* **17:** 754–755.

Kimura M. 1980. A simple method for estimating evolutionary rates of base substitutions through comparative studies of nucleotide sequences. *Journal of Molecular Evolution* **16:** 111–120.

Knowlton N. 1986. Cryptic and sibling species among the Decapod Crustacea. *Journal of Crustacean Biology* **6:** 356–363.

Lavane C, Preparata G, Saccone C, Serio G. 1984. A new method for calculating evolutionary substitution rates. *Journal of Molecular Evolution* **20:** 86–93.

Lin CW, Chan TY, Chu KH. 2004. A new squat lobster of the genus *Raymunida* (Decapoda: Galatheidae) from Taiwan. *Journal of Crustacean Biology* **24:** 149–156.

Machordom A, Macpherson E. 2004. Rapid radiation and cryptic speciation in galatheid crabs of the genus *Munida* and related genera in the South West Pacific: molecular and morphological evidence. *Molecular Phylogenetics and Evolution* **33:** 259–279.

Macpherson E. 1993. Crustacea Decapoda: species of the genus *Paramunida* Baba, 1988 (Galatheidae) from the Philippines, Indonesia and New Caledonia. In: Crosnier A, ed. *Résultats des Campagnes MUSORSTOM*, Vol. 10. *Mémoires du Muséum National d'Histoire Naturelle* **156:** 443–473.

Macpherson E. 1994. Crustacea Decapoda: Studies on the genus *Munida* Leach, 1820 (Galatheidae) in New Caledonia and adjacent waters with descriptions of 56 new species. In: Crosnier A, ed. Résultats des Campagnes MUSORSTOM, vol. 12. *Mémoires du Muséum National d'Histoire Naturelle* **161:** 421–569.

Macpherson E. 1996. Crustacea Decapoda: new records of species of the genera *Munida* Leach, 1820 and *Paramunida* Baba, 1988 (Galatheidae) from New Caledonia, with the descriptions of three new species. In: Crosnier A, ed. *Résultats des Campagnes MUSORSTOM*, vol. 15. *Mémoires du Muséum National d'Histoire Naturelle* **168:** 423–431.

Macpherson E. 2003. Some lithodid crabs (Crustacea: Decapoda: Lithodidae) from the Solomon Islands (SW Pacific Ocean), with the description of a new species. *Scientia Marina* **67:** 413–418.

Macpherson E. 2004. Species of the genus *Munida* Leach, 1820 and related genera from Fiji and Tonga (Crustacea: Decapoda: Galatheidae). In: Marshall BA, Richer de Forges B, eds. *Tropical Deep-Sea Benthos*, vol. 23. *Mémoires du Muséum National d'Histoire Naturelle* **191:** 231–292.

Macpherson E. 2006a. Galatheidae (Crustacea: Decapoda) from the Austral Islands, Central Pacific. In: De Forges BR, Justine JL, eds. *Tropical Deep-Sea Benthos*, vol. 24. *Mémoires du Muséum National d'Histoire Naturelle* **193:** 285–333.

Macpherson E. 2006b. New species and new occurrence of Galatheoidea (Crustacea, Decapoda) from New Caledonia. *Zoosystema* **28:** 669–681.

Macpherson E, Baba K. 2006. New species and records of small galatheids (Crustacea, Decapoda, Galatheidae) from the southwest and central Pacific Ocean. *Zoosystema* **28:** 443–456.

Macpherson E, Machordom A. 2005. Use of morphological and molecular data to identify three new sibling species of the genus *Munida* Leach, 1820 (Crustacea, Decapoda, Galatheidae) from New Caledonia. *Journal of Natural History* **39:** 819–834.

Mickevich MF, Farris JS. 1981. The implications of congruence in Menidia. *Systematic Zoology* **30:** 351–370.

Miller MC. 1969. Habits and habitats of opistobranch molluscs of British Solomon Islands. *Philosophical Transactions of the Royal Society of London Series B-Biological Sciences* **255:** 541–548.

Morrison CL, Harvey AW, Lavery S, Tieu K, Huang Y, Cunningham CW. 2002. Mitochondrial gene rearrangements confirm the parallel evolution of the crab-like form. *Proceedings of the Royal Society of London, Part B, Biological Sciences* **269:** 345–350.

Palumbi SR, Martin AP, Romano S, McMillan WO, Stice L, Grabowski G. 1991. *The simple fool's guide to PCR*. Honolulu: Special Publishing Department of Zoology, University of Hawaii.

Porter ML, Pérez-Losada M, Crandall KA. 2005. Model-based multi-locus estimation of decapod phylogeny and divergence times. *Molecular Phylogenetics and Evolution* **37:** 355–369.

Posada D, Crandall KA. 1998. MODELTEST: testing the model of DNA substitution. *Bioinformatics* **14:** 817–818.

Ptacek MB, Sarver SK, Childress MJ, Herrnkind WF. 2001. Molecular phylogeny of the spiny lobster genus *Panulirus* (Decapoda: Palinuridae). *Marine and Freshwater Research* **52:** 1037–1047.

Rodríguez R, Oliver JL, Marín A, Medina JR. 1990. The general stochastic model of nucleotide substitution. *Journal of Theoretical Biology* **142:** 485–501.

Schram FR. 1986. *Crustacea*. New York: Oxford University Press.

Schram FR, Feldmann RM, Copeland MJ. 1978. The late Devonian Palaeopalaemonidae and earliest decapod crustaceans. *Journal of Paleontology* **52:** 1375–1387.

Schubart CD, Conde JE, Carmona-Suarez C, Robles R, Felder DL. 2001. Lack of divergence between 16S mtDNA sequences of the swimming crabs *Callinectes bocourti* and *C. maracaiboensis* (Brachyura: Portunidae) from Venezuela. *Fishery Bulletin* **99:** 475–481.

Schubart CD, Diesel R, Hedges SB. 1998. Rapid evolution to terrestrial life in Jamaican crabs. *Nature* **393:** 363–365.

Swofford DL. 2002. *PAUP*: phylogenetic analysis using parsimony (* and other methods), Version 4*. Sunderland, MA: Sinauer Associates.

Tudge CC, Cunningham CW. 2002. Molecular phylogeny of the mud lobster and mud shrimps (Crustacea: Decapoda: Thalassinidea) using nuclear 18S rDNA and mitochondrial 16S rDNA. *Invertebrate Systematics* **16:** 839–847.

Wolff T. 1969. Fauna of Rennell and Bellona, Solomon islands. *Philosophical Transactions of the Royal Society of London Series B-Biological Sciences* **255:** 321–343.

Zariquiey Alvarez R. 1952. Estudio de las especies Europeas del gen. *Munida* Leach 1818. *Eos* **28:** 143–231.